NAVAL POSTGRADUATE SCHOOL

MONTEREY, CALIFORNIA

THESIS

AUTOMATED DETECTION OF A CROSSING CONTACT BASED ON ITS DOPPLER SHIFT

by

How, Whye Keong

March 2009

Thesis Advisor:	Daphne Kapolka
Co-Advisor:	Joseph Rice

Approved for public release; distribution is unlimited

THIS PAGE INTENTIONALLY LEFT BLANK

REPORT DOCUMENTATION PAGE			Form Approved OMB No. 0704-0188
Public reporting burden for this collection of information is estimated to average 1 hour per response, including the time for reviewing instruction, searching existing data sources, gathering and maintaining the data needed, and completing and reviewing the collection of information. Send comments regarding this burden estimate or any other aspect of this collection of information, including suggestions for reducing this burden, to Washington headquarters Services, Directorate for Information Operations and Reports, 1215 Jefferson Davis Highway, Suite 1204, Arlington, VA 22202-4302, and to the Office of Management and Budget, Paperwork Reduction Project (0704-0188) Washington DC 20503.			
1. AGENCY USE ONLY *(Leave blank)*	**2. REPORT DATE** March 2009	**3. REPORT TYPE AND DATES COVERED** Master's Thesis	
4. TITLE AND SUBTITLE Automated Detection of a Crossing Contact Based on Its Doppler Shift		**5. FUNDING NUMBERS**	
6. AUTHOR(S) How, Whye Keong			
7. PERFORMING ORGANIZATION NAME(S) AND ADDRESS(ES) Naval Postgraduate School Monterey, CA 93943-5000		**8. PERFORMING ORGANIZATION REPORT NUMBER**	
9. SPONSORING /MONITORING AGENCY NAME(S) AND ADDRESS(ES) N/A		**10. SPONSORING/MONITORING AGENCY REPORT NUMBER**	
11. SUPPLEMENTARY NOTES The views expressed in this thesis are those of the author and do not reflect the official policy or position of the Department of Defense or the U.S. Government.			
12a. DISTRIBUTION / AVAILABILITY STATEMENT Approved for public release; distribution is unlimited		**12b. DISTRIBUTION CODE**	

13. ABSTRACT (maximum 200 words)

The trade-off between false alarm and detection probability is a fundamental challenge in the automated detection of contacts in passive sonar systems. A common approach is the application of high-gain processing followed by successive classification criteria. Most classification schemes (e.g., matching of signature) are complex and tailored to specific target types. By contrast, the Doppler effect is readily observed in all contacts with discrete tonals and relative velocity to the receiver. This thesis demonstrates that the Doppler effect can be exploited to improve the detection process by filtering out contacts that do not exhibit these characteristics. Cross-correlation (matched filtering) of contact LOFARgrams with templates generated *in situ* with Doppler compression/dilation is used to achieve this. Velocity information and the range of the Closest Point of Approach (CPA) are estimated in the process. A detection algorithm is developed in MATLAB, and the radiated acoustic signatures of overflying airplanes are recorded at a ground station. In the analysis of six propeller and four jet airplanes, the program successfully identifies the passage of all six propeller airplanes with four incidences of false alarm, due in one case to a jet airplane. Velocity and range estimates are also within expected values.

14. SUBJECT TERMS Automated passive contact detection, Doppler shift, cross correlation, matched filter, velocity estimation, CPA range estimation			**15. NUMBER OF PAGES** 117
			16. PRICE CODE
17. SECURITY CLASSIFICATION OF REPORT Unclassified	**18. SECURITY CLASSIFICATION OF THIS PAGE** Unclassified	**19. SECURITY CLASSIFICATION OF ABSTRACT** Unclassified	**20. LIMITATION OF ABSTRACT** UU

NSN 7540-01-280-5500 Standard Form 298 (Rev. 8-98)
Prescribed by ANSI Std. Z39.18

THIS PAGE INTENTIONALLY LEFT BLANK

Approved for public release; distribution is unlimited

AUTOMATED DETECTION OF A CROSSING CONTACT BASED ON ITS DOPPLER SHIFT

How, Whye Keong
Major, Republic of Singapore Navy
B.Sc. (Hons) National University of Singapore, 1998

Submitted in partial fulfillment of the
requirements for the degree of

MASTER OF SCIENCE IN ENGINEERING ACOUSTICS

from the

NAVAL POSTGRADUATE SCHOOL
March 2009

Author: How, Whye Keong

Approved by: Daphne Kapolka
Thesis Advisor

Joseph Rice
Co-Advisor

Daphne Kapolka
Chair, Engineering Acoustics Academic Committee

THIS PAGE INTENTIONALLY LEFT BLANK

ABSTRACT

The trade-off between false alarm and detection probability is a fundamental challenge in the automated detection of contacts in passive sonar systems. A common approach is the application of high-gain processing followed by successive classification criteria. Most classification schemes (e.g., matching of signature) are complex and tailored to specific target types. By contrast, the Doppler effect is readily observed in all contacts with discrete tonals and relative velocity to the receiver. This thesis demonstrates that the Doppler effect can be exploited to improve the detection process by filtering out contacts that do not exhibit these characteristics. Cross-correlation (matched filtering) of contact LOFARgrams with templates generated *in situ* with Doppler compression/dilation is used to achieve this. Velocity information and the range of the Closest Point of Approach (CPA) are estimated in the process. A detection algorithm is developed in MATLAB, and the radiated acoustic signatures of overflying airplanes are recorded at a ground station. In the analysis of six propeller and four jet airplanes, the program successfully identifies the passage of all six propeller airplanes with four incidences of false alarm, due in one case to a jet airplane. Velocity and range estimates are also within expected values.

THIS PAGE INTENTIONALLY LEFT BLANK

TABLE OF CONTENTS

LIST OF FIGURES

THIS PAGE INTENTIONALLY LEFT BLANK

LIST OF TABLES

THIS PAGE INTENTIONALLY LEFT BLANK

ACKNOWLEDGMENTS

My learning journey at the Naval Postgraduate School and the completion of this thesis would not have been possible without the support of the following people:

First and foremost, special thanks to my lovely wife, Mei Wah, for her unwavering support, love and patience. She is my pillar of strength and source of inspiration. Thank you for the sacrifices you have made and for taking such good care of our beautiful children, Hazel and Herrmann.

To my thesis advisor, Professor Daphne Kapolka, for the opportunity to take on the project and for your patience and guidance in keeping me on track throughout the project. Thank you for teaching me to learn and think simply.

To my co-advisor and second reader, Professor Joe Rice, for talking to me about the Seaweb Networks and commenting on my thesis. Thank you, sir.

And lastly, to all the professors, friends and classmates for making my stay at NPS a memorable one.

THIS PAGE INTENTIONALLY LEFT BLANK

I. INTRODUCTION

A. BACKGROUND

The Seaweb program uses a network of underwater acoustic modems to communicate without the use of cables. These networks, once laid, provide round-the-clock presence in the area of interest. Recent work explores the possibility of using these underwater modems for a surveillance role in shallow waters and harbor entries. To achieve this, the components used in the existing network may need to be supplemented with additional hardware and software to sense the passive acoustic signature generated by maritime vessels. In addition to the provision of continuous monitoring of the environment around the modem for passing vessels, the collected acoustic signatures or shorter contact reports can also be transmitted ashore for analysis.

In a multiple-sensor network, the amount of information that needs to be processed by the onshore operator increases with the number of sensors. Even before analysis of any collected signature can be done, the validity of a contact as a maritime vessel, as opposed to other competing noise sources, has to be determined. Automation of detection is the obvious solution in a contact-rich environment. However, the fundamental trade-off between the probability of detection and the probability of false alarm remains the challenge in the design of the automation logic and system. Setting too low a threshold results in a high false-alarm rate, while the converse results in a high chance of missed detection of an otherwise valid contact.

The traditional detection system trigger is commonly based on the received signal being above a predetermined threshold, which is usually determined by operational requirements. The selection of an appropriate threshold that does not result in too many false alarms then becomes the challenge. Techniques such as the Neyman-Pearson criterion may be used to compute the threshold for a desired false-alarm rate (Ziomek, 1994). Alternatively, the use of a second independent property of the contact of interest

can serve as a second-level filter to weed out false alarms before declaring a detection decision. This thesis explores the use of the Doppler effect, which is visible in moving contacts with narrowband frequency components, as a second-level filter to decrease the probability of false alarm in the automated triggering mechanism. In addition, the velocity and passing range, which are important contact parameters, are estimated from the Doppler shift exhibited by the moving contact.

B. RESEARCH MOTIVATION

> *The trade-off between the false alarm and detection probability is fundamental in radar and sonar. (Chevalier, 2002)*

A common approach to the detection of passive contacts is to apply high-gain processing to the raw signal to increase the signal-to-noise (SNR) ratio. The processed signal is then compared to a threshold value.

Statistically, if the difference between the contact's mean signal level and that of the background noise is big, the probability of false alarm (P_{fa}) can be reduced by setting the detection threshold higher without significantly increasing the probability of non-detection (P_{nd}) of a true contact. However, in cases where this difference is small (as in case of a weak contact), the level at which the threshold is set involves in a trade-off between reducing P_{fa} and P_{nd}.

Many of the currently used classification methods are complex and mostly aimed at specific contacts (e.g., matching of contact signature). While the use of the Doppler shift is well established in the fields of active radar and active sonar for deriving velocity information on the contact, it is not as straightforward in the passive case due to the lack of a known transmitted waveform with which to cross-correlate the return echo. However, the Doppler effect is still an attractive classification criterion for the detection of moving contacts as it is prevalent in all moving contacts showing tonal lines. The objective of this research is to demonstrate the possibility of using the Doppler effect to discriminate legitimate

moving contacts from background clutter, which will in turn allow the threshold for auto detection to be set closer to the noise floor without significantly increasing the false-alarm rate.

C. RESEARCH SUMMARY

This thesis is limited to the demonstration that the Doppler effect from moving contacts can be used to discriminate a moving contact with distinct tonals from competing sources of noise. The velocity and range of the contact are also estimated to a limited degree of accuracy.

The theoretical framework of the tactical trade-off between probability of detection and probability of false alarm is first developed. The physics of the Doppler effect are then presented. Incorporation of the Doppler effect as a second-level filter is demonstrated as a means for lowering the detection threshold without increasing the probability of false alarm.

The Doppler effect is commonly and routinely used in the time-frequency analysis of contacts in passive sonar. It is apparent on a spectrogram and is readily identifiable by a trained operator. As the goal of this research is to automate the process, the challenge is to develop a signal processing algorithm that not only recognizes the Doppler effect when it is present, but also analyzes the Doppler curve as a trained operator would do. Once this algorithm is programmed, a suitable candidate target has to be selected to test the fidelity of the algorithm.

Acoustic data of overflying airplanes on approach for landing at the Monterey Peninsula Airport were collected at a land station against a background consisting of natural and manmade noise, such as automobile traffic. An algorithm was developed and programmed in MATLAB to search the collected data and detect a passing airplane by identifying the Doppler effect. The results were compared against airport records to check the fidelity of the program. The algorithm is shown to be extremely successful in discriminating between loud contacts which do not exhibit an easily discerned Doppler shift (jet airplanes) *vis-á-vis* those exhibiting a clear Doppler shift (propeller planes).

Finally, recommendations for further work to apply the algorithm to an underwater environment and passive sensing systems are presented.

II. THEORY

A. THE TACTICAL TRADE-OFF BETWEEN PROBABILITY OF DETECTION AND PROBABILITY OF FALSE ALARM – A STATISTICAL ANALYSIS

1. Detection Performance

The detection process involves a decision about the presence of a contact through the processing of its signal (acoustic, radar returns, etc.) against the ambient noise of the background medium. A detection decision is declared if the received signal level exceeds a predetermined threshold. In the sonar context where logarithmic quantities are used, the detection decision can be represented by the following condition in the sonar equation:

Signal – Noise + Gain > Threshold. Eq. 2.1

This "signal" is not limited to a time domain or frequency domain signal but can be extended to mean any measurable output of the sensor system.

The performance of a system is characterized by two statistics, namely:

Probability of Detection, P_d, defined as the probability that a processed signal exceeds the predetermined threshold when the contact of interest is present.

Probability of False Alarm, P_{fa}, defined as the probability that a processed signal exceeds the predetermined threshold even though no contact of interest is actually present.

It is immediately obvious that the correct selection of the predetermined threshold is the key to the system's performance. A conservative decision criterion designed to minimize false alarms translates to setting a high threshold. This means that only strong signals result in a positive detection call, giving a

small $P_{fa,}$ and a correspondingly lower P_d. On the other hand, an aggressive criterion designed to maximize the probability of detection would use a low threshold to increase P_d at the expense of a high P_{fa}. In Figure 1, the "signal" being evaluated is the power output as a function of time. A lower threshold increases the number of false alarms triggered by noise spikes, while a high threshold reduces the number of false alarms by noise spikes but also results in legitimate signals being missed.

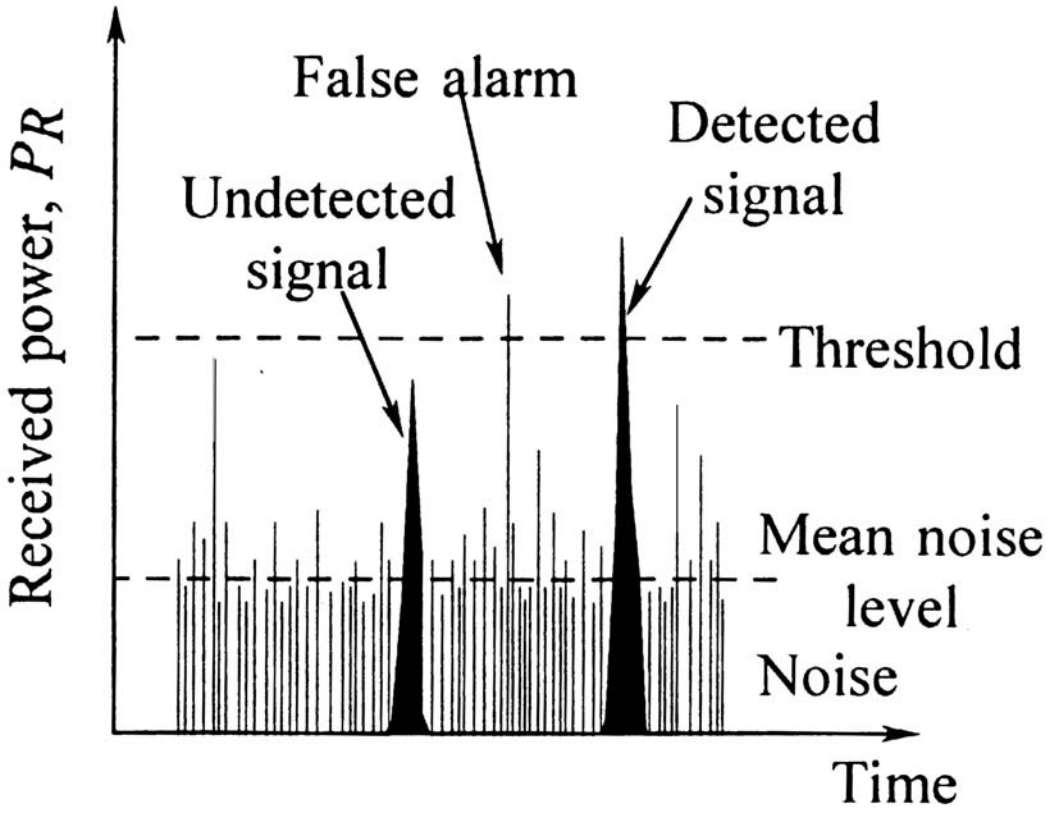

Figure 1. Illustration of Effects of Varying Threshold on Detection and False Alarm (From: Wagner, Mylander, & Sanders, 1999)

2. Optimizing Performance

In both sonar and radar applications, optimization of system performance is done such that P_d is maximized for a given upper limit of P_{fa}. The aim is to find a balanced and acceptable threshold level (false-alarm rate). This decision is influenced by, among other factors, the operational imperatives of the system favoring one criterion or another. In some cases (e.g., detection of enemy submarines), a non-detection might have fatal consequences, whereas false alarms have less serious consequences, such as a waste of time and effort. Here, an aggressive decision criterion designed to maximize the probability of detection would be favored.

To examine the trade-off between the probability of detection and the probability of false alarm in more detail, consider a case where the received signal is Gaussian regardless of whether a contact is present or not. The actual statistics of the received signal in both cases depend on the nature of the signal of interest, the noise, and the way in which the raw signal is measured. However, any assumed statistics serve to illustrate the trade-off. In the discussion which follows, let $s_{rx}(t)$ be the amplitude of the received signal. The signal due to the contact of interest is $s(t)$, and the selected detection threshold against which the signal is compared for a detection decision is T. Assume further that the noise-only signal is stationary and given by $n(t)$ which has a mean of μ_N and a variance σ^2. If the contact is present, assume that the received signal has a mean of μ_{S+N} and a variance of σ^2. The following two cases may occur.

a. Contact is Absent

In the case where there is no contact of interest in the environment, the only signal received by the sensor is Gaussian noise, $n(t)$. Hence, $s_{rx}(t) = n(t)$ where $s_{rx}(t) \sim N(\mu_N, \sigma^2)$. Since there is no contact, any detection decision is a false alarm. The following equation applies and is illustrated in Figure 2.

$$P_{fa} = \Pr\{s_{rx}(t) \geq T \mid s_{rx}(t) \sim N(\mu_N, \sigma^2)\}$$
$$= \frac{1}{\sigma\sqrt{2\pi}} \int_{T}^{+\infty} \exp\left(-\frac{(x-\mu_N)^2}{2\sigma^2}\right) dx$$
$$= 1 - \Phi\left(\frac{T-\mu_N}{\sigma}\right) \qquad \text{Eq 2.2}$$

where Φ is the cumulative normal function.

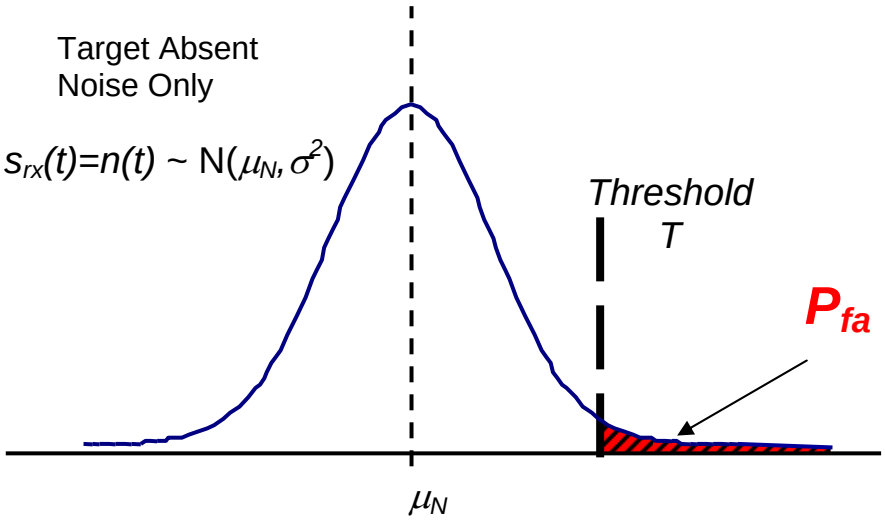

Figure 2. Illustration of the Noise-Only Case

b. Contact is Present

When a contact of interest is present, the received signal is the sum of the signal from the contact *s(t)* and the noise *n(t)*. The probability of detection is thus the probability of the sum of signal and noise exceeding the threshold, where

$s_{rx}(t) = s(t) + n(t)$ and $s_{rx}(t) \sim N(\mu_{N+S}, \sigma^2)$

$$P_d = \Pr\{s_{rx}(t) \geq T \mid s_{rx}(t) \sim N(\mu_{N+S}, \sigma^2)\}$$
$$= \frac{1}{\sigma\sqrt{2\pi}} \int_T^{+\infty} \exp\left(-\frac{(x-\mu_{N+S})^2}{2\sigma^2}\right) dx$$
$$= 1 - \Phi\left(\frac{T-\mu_{N+S}}{\sigma}\right) \qquad \text{Eq 2.3}$$

This is illustrated in the following figure.

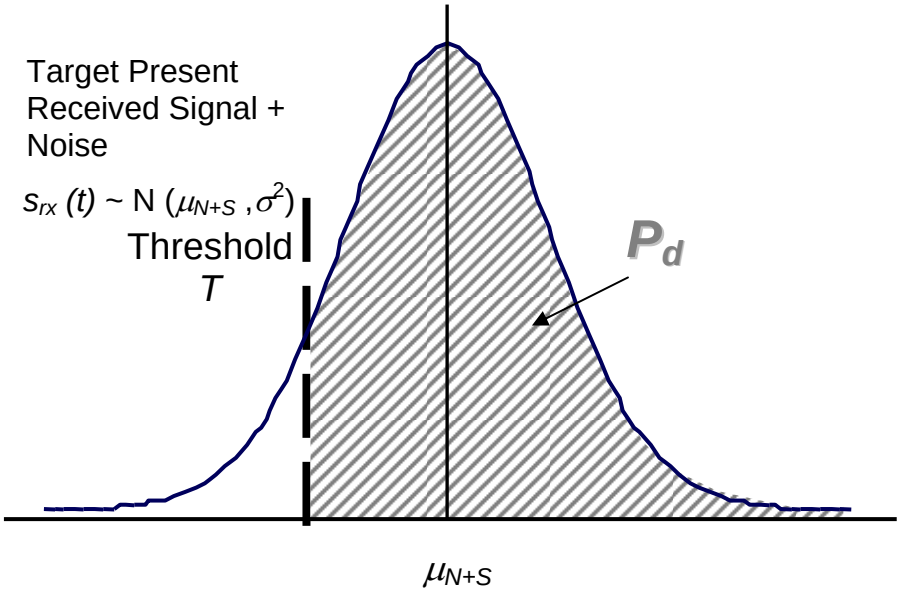

Figure 3. Illustration of Target+Noise Case

Putting both the above cases together, the following illustration, with both of the above probability distributions, shows the situation encountered by the sensor in the presence of noise. There will inevitably be false alarms

caused by noise only regardless of the selected threshold and the link between P_d and P_{fa} can clearly be seen.

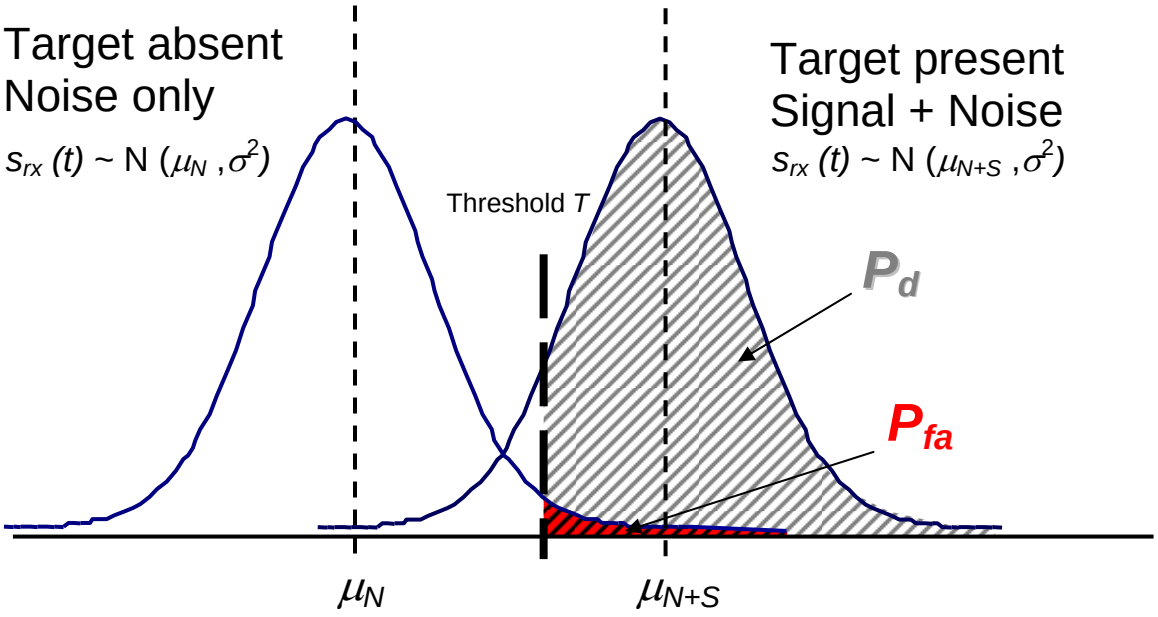

Figure 4. Sensor Detection in Background with Noise

If the "costs" associated with false alarms and missed detection can be quantified and are known, an optimized threshold can be computed mathematically (Washburn, 1996).

Summarizing all possible cases results in the flowing matrix:

	Target Present	Target Absent
Sensor indicates Target Present	P_d (True Positive)	P_{fa} (False Alarm / False Positive)
Sensor indicates Target Absent	1- P_d (Missed Detection / False Negative)	1- P_{fa} (True Negative)

Table 1. Target Matrix

3. Receiver Operating Characteristics (ROC) Curves

The ROC curve is a plot of P_d against P_{fa} for a sensor system. It was first used during World War II for analysis of radar signals before being employed in signal detection theory (Green and Swets, 1966). These curves show the trade-off between P_d and P_{fa} for different signals of interest and noise statistics as the detection threshold is changed.

From Equations 2.2 and 2.3, $P_d = 1 - \Phi\left(\frac{T - \mu_{S+N}}{\sigma}\right)$ and $P_{fa} = 1 - \Phi\left(\frac{T - \mu_N}{\sigma}\right)$. Let the normalized threshold be $x = \frac{T}{\sigma}$. The equations for the probability of detection and false alarm can then be written $P_d = 1 - \Phi\left(x - \frac{\mu_{S+N}}{\sigma}\right)$ and $P_{fa} = 1 - \Phi\left(x - \frac{\mu_N}{\sigma}\right)$. This makes it clear that the difference in the probability of detection and the probability of false alarm depends on the difference in the values of $\frac{\mu_{S+N}}{\sigma}$ and $\frac{\mu_N}{\sigma}$ as well as on the choice of threshold. The detection index is defined in terms of the difference of these values as $d = \left(\frac{\mu_{S+N} - \mu_N}{\sigma}\right)^2$. It is a measure of the signal-to-noise ratio. Higher values of the detection index yield better detection performance for a given threshold value. At the same time, for a given detection index, P_d and P_{fa} increase with lower threshold values. These relationships are shown in the ROC curve below.

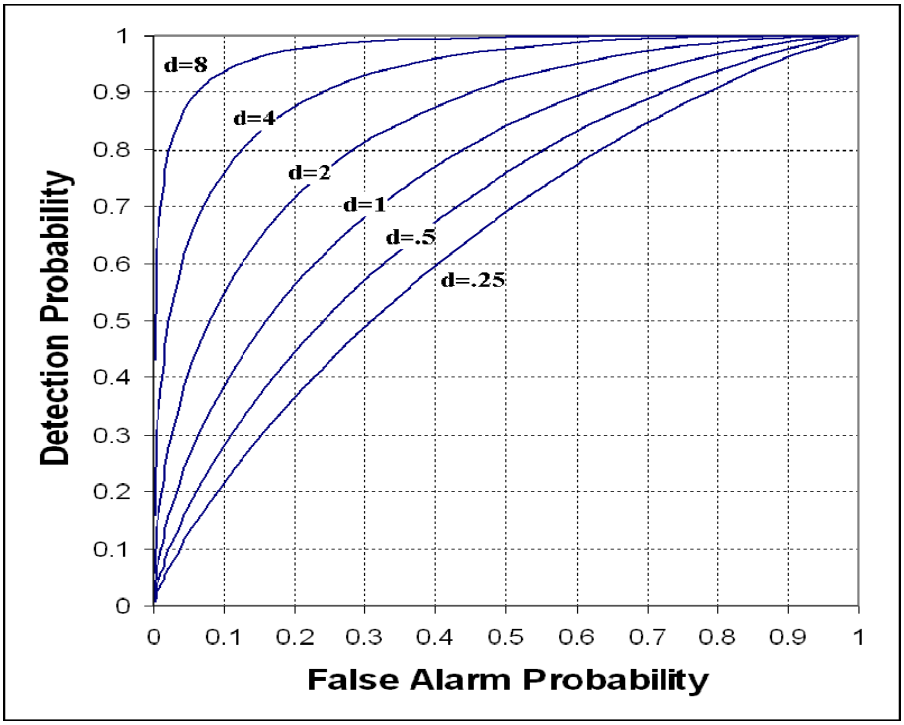

Figure 5. Generic ROC Curves

B. THE DOPPLER EFFECT

The Doppler effect refers to a shift of the apparent signal frequency caused by the relative motion of the source and receiver. Valuable information about the contact's trajectory can be derived from its Doppler shift.

1. Near the Closest Point of Approach (CPA)

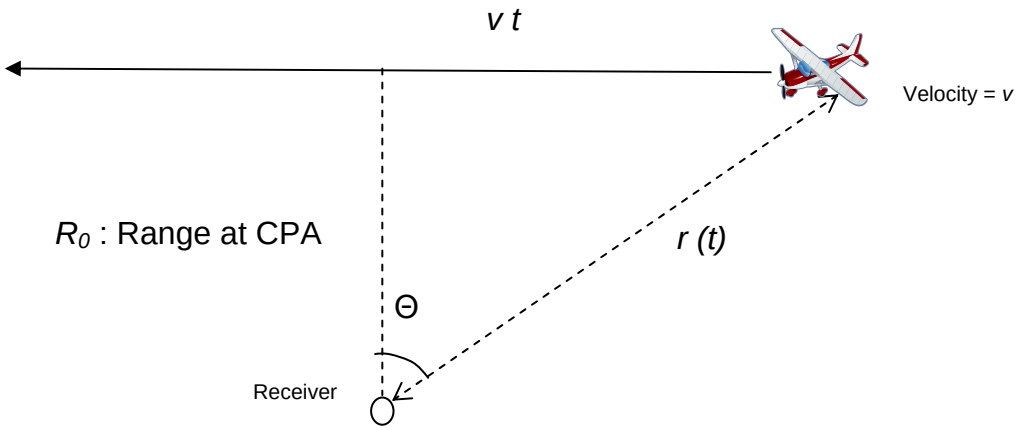

Figure 6. Passage of Airplane through CPA

Consider the above figure, illustrating an airplane flying by a stationary receiver with constant velocity, *v*. If the time of CPA is taken to be zero, the component of the plane's velocity towards the receiver along the line of sight at time *t* is given by:

$$v_{LOS} = v\sin\theta = v\frac{vt}{r(t)} = \frac{v^2 t}{\sqrt{(vt)^2 + R_0{}^2}}\ . \qquad \text{EQ 2.4}$$

The apparent frequency received at the receiver at any time,

$$f = \frac{f_0}{1-\frac{v_{LOS}}{c}} = \frac{f_0(1+\frac{v_{LOS}}{c})}{(1-\frac{v_{LOS}}{c})(1+\frac{v_{LOS}}{c})} = \frac{f_0(1+\frac{v_{LOS}}{c})}{1-(\frac{v_{LOS}}{c})^2} \qquad \text{EQ 2.5}$$

where f_0 is the frequency received at CPA when the plane has zero velocity along the line of sight and *c* is the speed of sound in the medium.

For $c >> V_{LOS}$, equation 2.5 simplifies to the following :

$$f = f_0 (1 + \frac{v_{LOS}}{c}) \quad .$$ EQ 2.6

Rearranging and differentiating with respect to *t* yields :

$$\frac{d v_{LOS}}{d t} = \frac{d f}{d t} (\frac{c}{f_0}) \quad .$$ EQ 2.7

When the plane is close to CPA, $\Theta << 1$, hence

$$v_{LOS} = v \sin\theta \cong v\theta \cong v \tan\theta = -v\frac{vt}{R_o} \quad ,$$ EQ 2.8

where t is negative before CPA and positive after.

Substitution of Eq 2.8 into Eq 2.7 yields :

$$\frac{d v_{LOS}}{d t} = - \frac{v^2}{R_o} = \frac{d f}{d t} (\frac{c}{f_0})$$

$$\frac{d f}{d t} = - \frac{v^2}{R_o} (\frac{f_0}{c}) \, .$$ EQ 2.9

The rate of change of frequency as the contact passes through CPA is proportional to its speed and inversely proportional to distance. Therefore, a measurement of the rate of change of frequency near CPA can be used to estimate the range at CPA**.**

2. Away From the CPA

The received frequency of the contact approaches an asymptotic value when it is far away; hence, the center frequency can be computed from the opening and closing asymptotic values:

$$f_o = \frac{f_u + f_L}{2}, \qquad \text{EQ 2.10}$$

where fu is the closing (upper) frequency asymptotic value and fL is the opening (lower) frequency. The Doppler shift is then given by:

$$\Delta f = f_u - f_o = f_0 \frac{v}{c}. \qquad \text{EQ 2.11}$$

Rearranging, the speed of the contact, *v,* gives:

$$v = \frac{c \Delta f}{f_0}. \qquad \text{EQ 2.12}$$

Through the measurement of f_U and f_L, the velocity can be determined, which can then be substituted back into EQ 2.9 to determine the CPA range R_0.

3. Doppler – Range Ambiguity

The recorded pressure vs. time signal in the time domain is a noisy waveform that conveys little information to the human eye and yields little information for easy analysis. Therefore, a Discrete Fourier Transform (DFT) is used to transform it into its corresponding representation in the frequency domain so that the amplitude of the component sinusoids can be extracted. However, the two parameters, time and frequency, are conjugated by the process of Fourier transform.

The process of transformation involves first multiplying the signal by a smooth curve (typically a Hamming window), following which, the DFT is taken. However, if the DFT for the entire sample is taken as one long data sequence, the variance of the noise can be large, making it difficult to observe the frequency components of the signal of interest. It is common practice instead to break the input signal into many smaller segments. Each of these segments is multiplied by the Hamming window, run through the DFT, and the resulting frequency spectra are then averaged to form a single frequency spectrum. This process of averaging reduces the noise variance, allowing interesting features of the signal to become prominent. However, the length of the DFT translates to frequency resolution. By taking segmented parts of the original signal, we trade frequency resolution to provide more ”averages.” For a finite signal, the number of averages is governed in turn by the length (integration time) of each segment. Hence, if we desire a spectrum of high-frequency resolution, longer segments (longer integration time) would be required and vice versa. This results in a Frequency (Doppler) - Time (Range) ambiguity that is inherent in our analysis.

C. CROSS-CORRELATION AND IMAGE DETECTION

The concept of correlation involves the mathematical operation of two signals (received signal and template waveform) to generate a third signal.

$$f(t) \star g(t) = \int_{-\infty}^{\infty} f^{*}(t)\, g(t+\tau)\, dt \qquad \text{EQ 2.13}$$

When the two signals are different, the process is known as cross-correlation. The following is a simple illustration of the cross-correlation process. For two finite length real discrete sequences, *x(n)* and *y(n)*, the cross-correlation is defined as :

$$\dot{R}_{xy}(m) = \sum_{n=0}^{N-1} x(n)\, y(n+m) \qquad \text{EQ 2.14}$$

x(n) is a received signal within which we wish to look for a certain waveform, *y(n)*, the template waveform. This is achieved by taking the sum of the product of *x(n)* and *y(n+m)* for different values of *m* to give a corresponding value of R_{xy}. By ”shifting” *y(n)* by delay *m*, the amplitude of R_{xy} at each ”sampling position” is therefore a relative measure of how closely a particular segment of the received waveform *x(n)* resembles the template waveform *y(n)*. When plotted, a peak occurs in R_{xy} if the template waveform is present in the received signal *x(n)*. Extending the same principle, correlation can be used to look for a known pattern in an image. The pattern is correlated to different segments of the main image or different sample images are correlated to the main image to find the location of the best match or a sample of the best match.

Cross-correlation involving a template signal is also known as matched filtering.

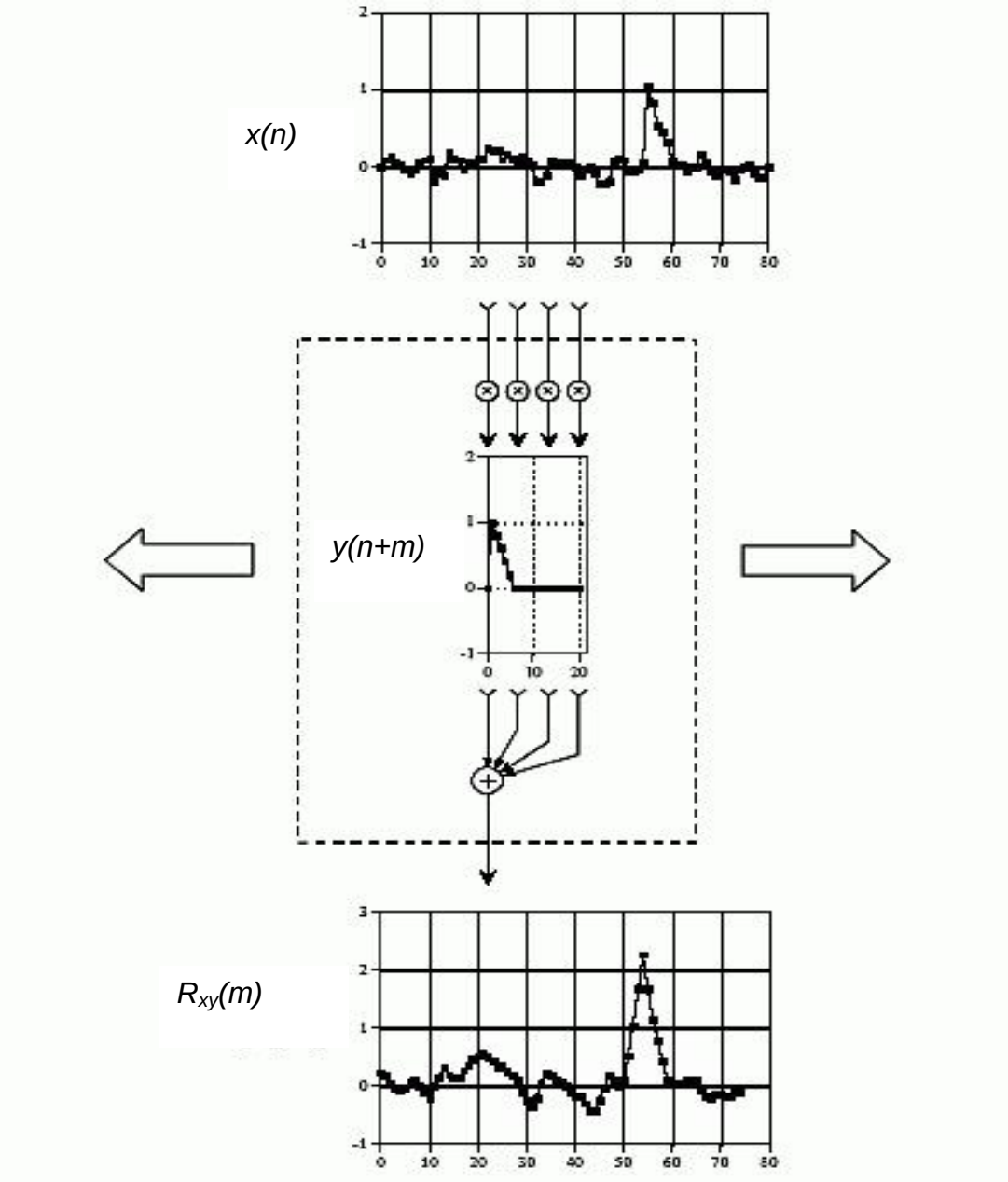

Figure 7. Illustration on Concept of Cross-correlation (After: Smith, 1997)

III. EXPERIMENTAL AND COMPUTER PROGRAM

A. DATA COLLECTION

1. Choice of Data Source

For consistency with the assumptions made in the development of the equations introduced in Chapter II, the contact should have a constant course and speed as it passes CPA. To establish ground truth, the contact should also be identifiable. In addition, the contact should also have tonals with Doppler shifts in the mid-frequency range, where they are best observable. For an assessment of the accuracy of the program's estimate of velocity and range, the velocity and CPA should also be known.

It is fortuitous that the Naval Postgraduate School (NPS) is located near the flight path of the Monterey Peninsula Airport. This makes it convenient to make recordings of airplanes passing overhead on their final approach to land. These airplanes meet the above criteria as they make minimal course and speed changes during this phase of flight. Distinct tonals from the propeller airplanes are present in the 100–1000 Hertz (Hz) frequency range. As will be shown in the next paragraph, the range at CPA can be estimated. The airplane's velocity can be deduced based on the identity and type of airplane. These conditions made them good candidate targets for this study.

2. Location of Recording

An hour of recording was conducted on 07 Aug 2008 from the top of the tower of Herrmann Hall, NPS. The airplanes were either flying the final approach of the Instrument Landing System (ILS) glide slope of the Monterey Peninsula Airport's runway 10R (depicted by dotted lines in the aerial photo) or on the visual approach to the parallel runway 10L.

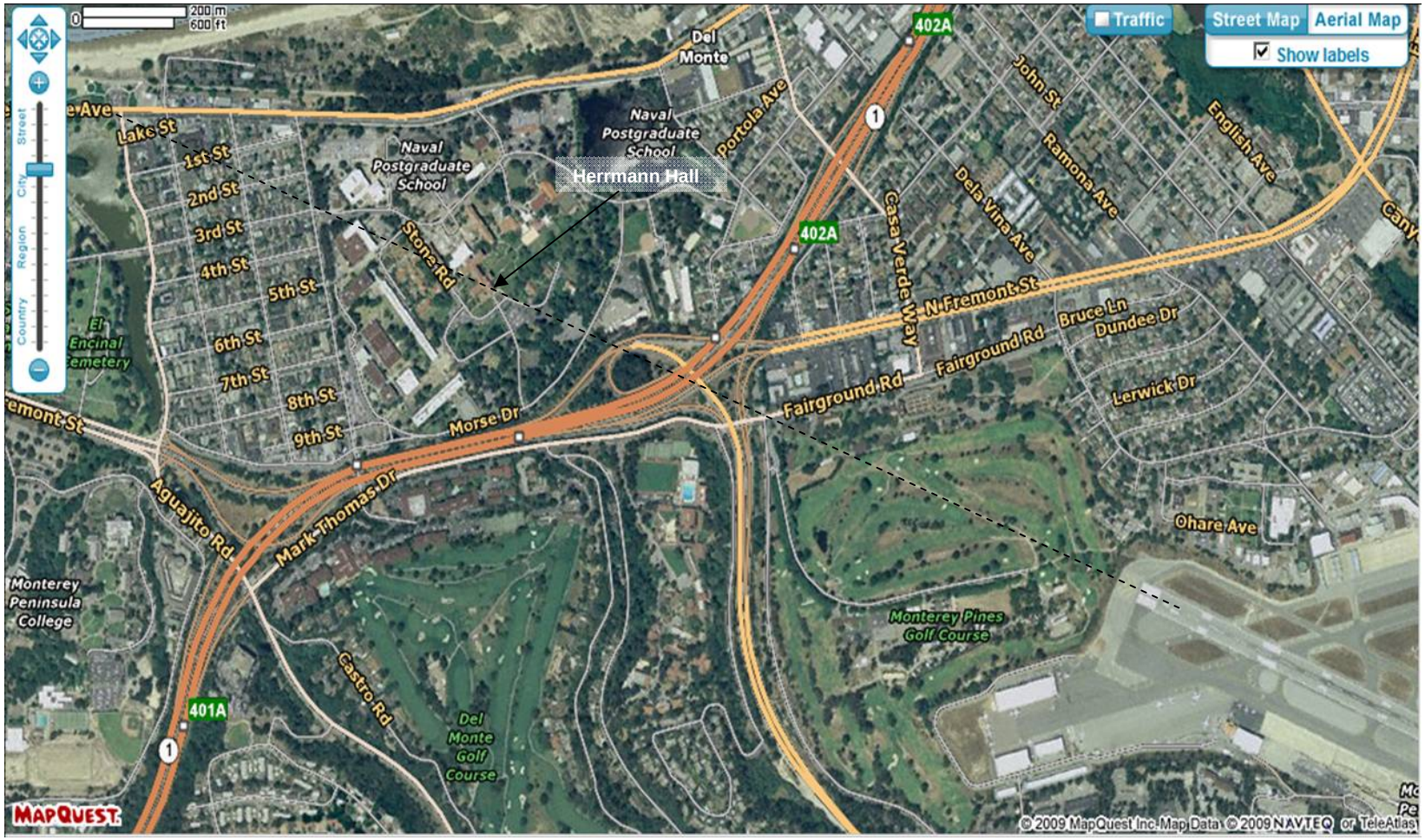

Figure 8. Aerial Photo of the Naval Postgraduate School and Surroundings (From: Mapquest, n.d.)

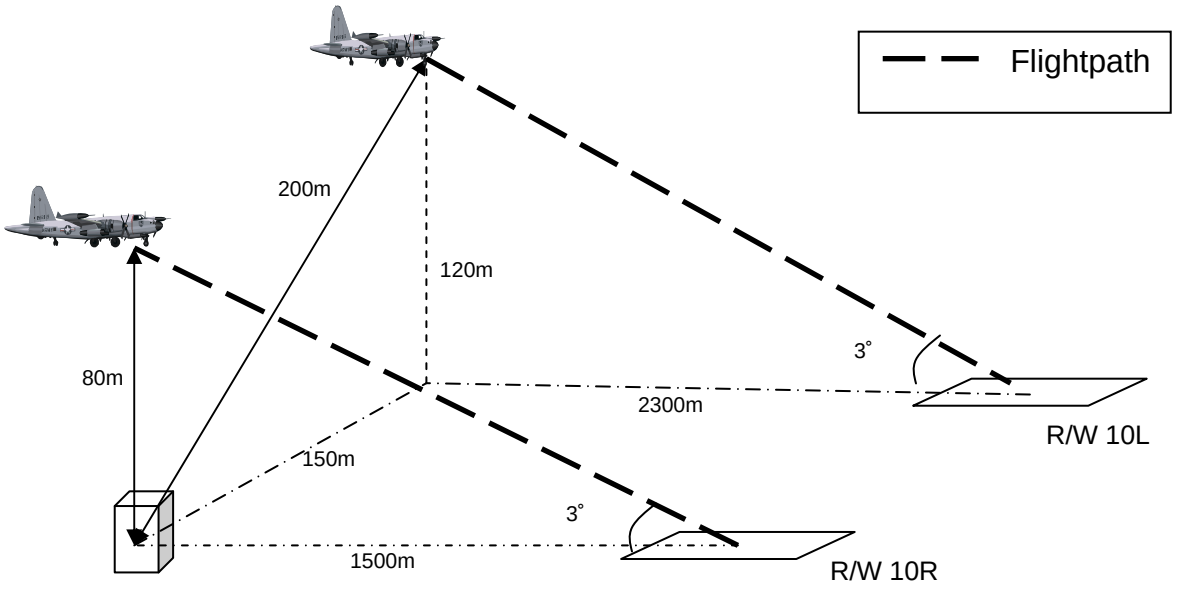

Figure 9. Schematic Diagram of Target Track Relative to Fixed Observing Station

Based on measurements taken from the above aerial photo, the distance between the tower of Herrmann Hall and the runway is estimated to be 1.5 kilometers (km). For airplanes flying overhead on the 3˚ ILS glide slope, a passing distance of 80 meters (m) between the receiver microphone and airplane at CPA is approximated. Airplanes on approach to the parallel runway 10L are estimated to have a passing distance of 200 m.

3. Equipment and Setup

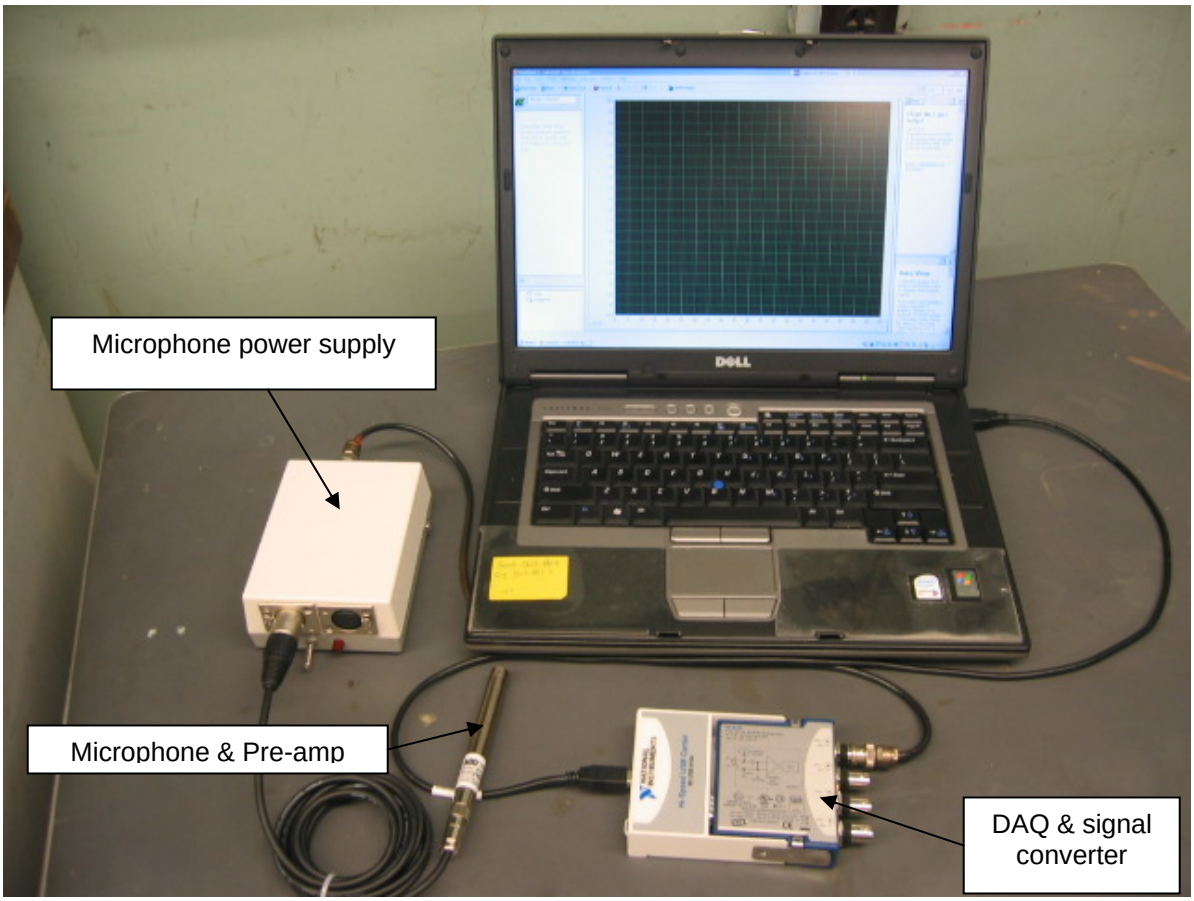

Figure 10. Photograph of Equipment Setup used in Recording

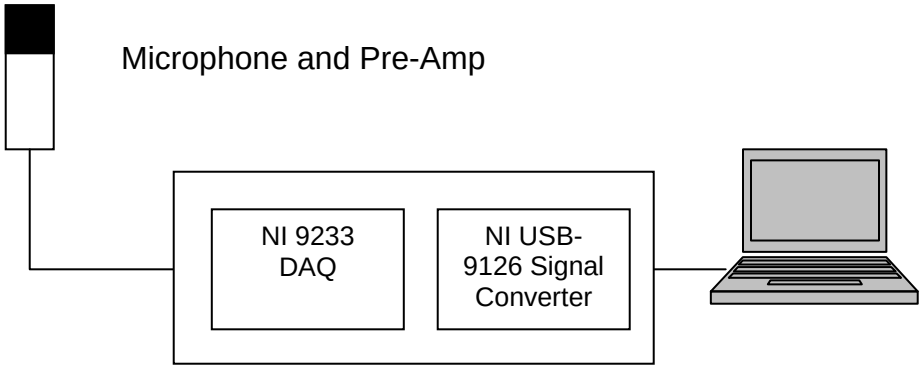

Figure 11. Graphical Representation of Equipment Setup

The equipment used for the recording is listed as follows. The technical specifications are included in Appendix A.

a. ACO Pacific Microphone. – Cartridge model 7046 & 4012 – $\frac{1}{2}$ inch Preamplifier

b. National Instrument NI9233 Dynamic Signal Acquisition modules with USB carrier.

c. Dell D820 Laptop

4. Processing of Collected Data

Acoustic data are processed and stored in the National Instruments' (NI) proprietary Technical Data Management - Streaming (.tdms) file format using the included NI LABVIEW SIGNAL EXPRESS version 2.5 software. This is subsequently converted and stored as an ASCII text file (.txt) using LABVIEW Express' built-in file converter prior to the commencement of the post-analysis phase.

B. MATLAB COMPUTER PROGRAM – AUTO DOPPLER DETECTOR.M

1. Program Overview

MATLAB Program 'auto_Doppler_detector.m' was written to analyse the recorded data. The purpose of the program is to detect airplane passages and to determine if they are propeller airplanes through analysis of the detected energy level in conjunction with the presence of Doppler shift. The collected raw signal (uncalibrated sound pressure) is input as a .txt file. In addition to flagging the propeller airplanes that exhibit Doppler shifts, the program also returns the time of CPA, frequency of the strongest tonal, and an estimate of both the velocity and range at CPA. On completion of analysis, plots containing pertinent information on the passage and a summary of the detected peaks are produced to form the post-analysis report.

2. Program Structure

The structure of the program is represented in the following flow chart.

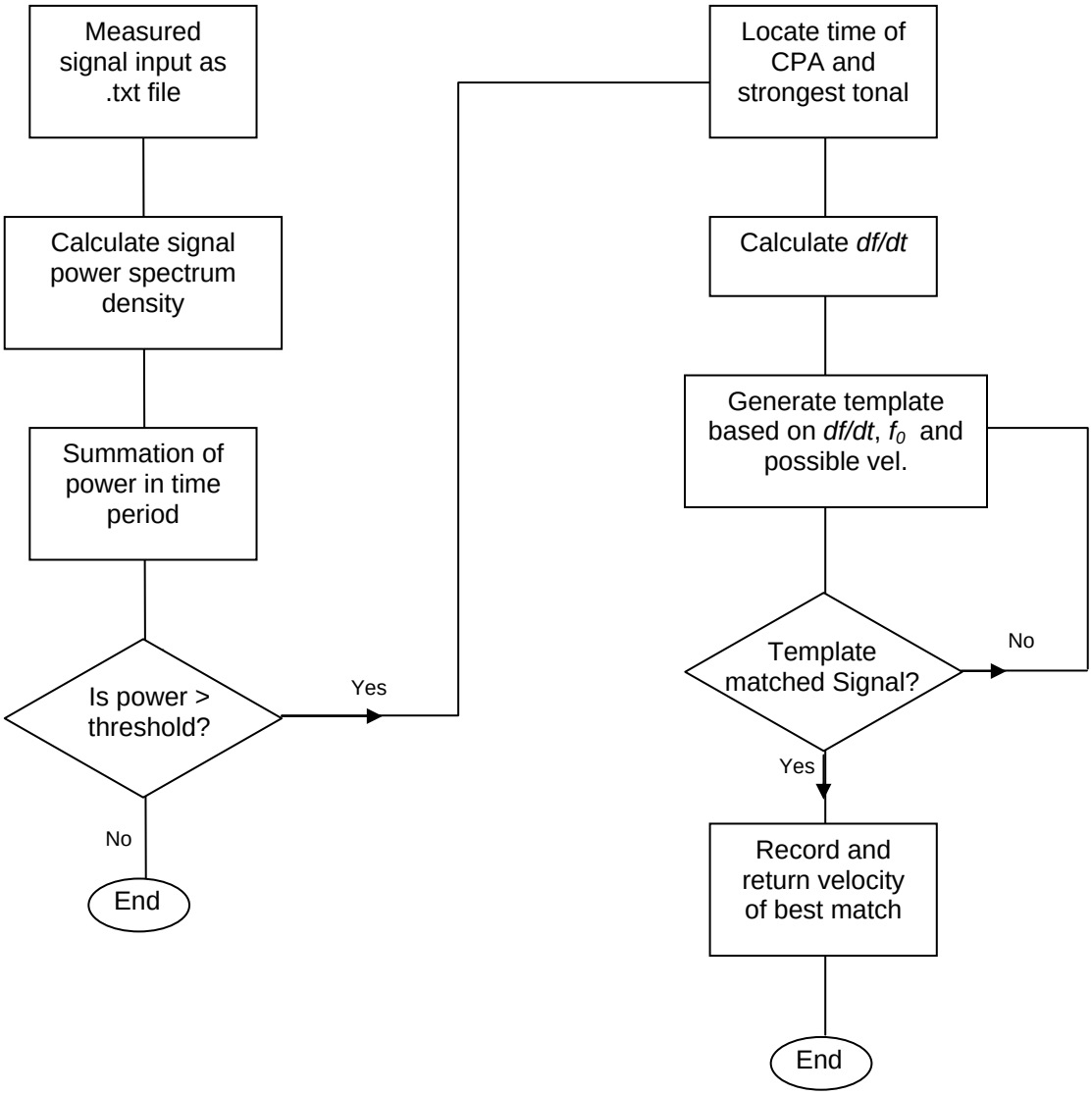

Figure 12. Flow Chart of Program auto_Doppler_detector.m

The power spectral density of the time domain input signal is estimated using the MATLAB built-in function ‘pwelch.m’ via Welch's method. By summing

the total energy in the time bands, the program detects the presence of an airplane passage or increase in sound energy and flags the corresponding time period for analysis.

A search is conducted within the flagged time period for the time with the highest energy. This time is associated with the time of CPA, t_{CPA}, based on the assumption that the energy of a passing airplane is highest at CPA.

The strongest tonal at time t_{CPA} is identified and its frequency, f_0 is noted. This tonal forms the basis for Doppler analysis. The corresponding strongest tonals in the preceding time (before t_{CPA}) and proceeding time (after t_{CPA}) within a frequency span of Δf are likewise determined. Δf is calculated using Eq 2.11, using the highest expected contact speed. Through the tracking of these tonals during the passage of the target near CPA, the rate of change of frequency with respect to time is computed.

Cross-correlation of the recorded signal's tonal in the region of CPA against synthetically generated Doppler profiles of a range of hypothetical velocities with the determined *df/dt* is then carried out. The result of the cross correlation factor, R_{xy} at various velocities is tabulated. A high R_{xy} value is an indication of a good match and can thus be used to deduce the presence of the Doppler curve. CPA range is then computed based on the velocity of best match.

3. Considerations in Design of the Program

As the program is envisaged to reside in an underwater modem, the size of the program and the speed in which the results are obtained are considerations in its design. This led to the rejection of using pre-generated template signals of all possible contact velocities and passing ranges stored for correlation against the recorded signal. The library of templates covering all possible scenarios would require large storage space and accessing them would slow down the program due to their sheer number and time required to load them. Instead, to achieve a small memory requirement, templates are generated

in situ based on the measured frequency rate change and f_0. This removes the need for any stored templates and greatly reduces data processing time. The MATLAB function 'generate_template.m' generates the required templates. This program, as well as all others written to support this thesis are provided in the appendices.

4. Underlying Assumptions and Significant Decisions

The accuracy, fidelity and robustness of any algorithm hinges on the assumptions made and the parameter estimate at key decision points. The underlying assumptions and their implications are discussed as follows:

a. Estimate of df/dt Near CPA

In order to keep the assumption in Eq 2.8 valid, ($\Theta << 1$), the number of differences that can be taken to provide an estimate of *df/dt* in the vicinity of CPA was limited to one sample point before and after CPA in this study, i.e., *df/dt* is an average of only two estimates. This is due to the close range, R_0, of 80 m between the airplane and receiver microphone, high speed of the planes - between 30 to 70 metres per second (m/s) – and uncertainty in the estimate of CPA time t_0 (1 second) as a result of conducting the analysis in the frequency domain. This calculation is illustrated in Figure 13.

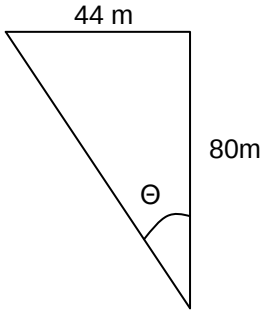

For $\sin\Theta \approx \Theta \approx \tan\Theta$ (accurate to 1st decimal), $\Theta_{max} \approx 28.65^{\circ}$. For an airplane travelling at 50m/s, to keep $\Theta < \Theta_{max}$, the period of 'valid time' is 0.88 second before and after CPA.

Figure 13. Calculation of "Maximum Valid Time Period"

b. Tracking the Doppler Shift and Calculation of df/dt

To calculate the rate of change of frequency in the vicinity of CPA, the program “looks” for the strongest tonal within a frequency range in the vicinity of f_0 in the time periods adjacent to CPA. The assumption that these strongest tonals are in fact due to the Doppler shift of f_0 subjects the analysis to possible error. Spurious noise or other signals from the contact with a higher amplitude than f_0 could lead to the misidentification of the tonal line and an error in the estimation of *df/dt*. This “risk” is mitigated in the program by limiting the frequency range over which the search is conducted.

c. Flagging Inadmissible df/dt

The sign of *df/dt* for a true Doppler shift will always be negative as the contact proceeds through CPA. This property is used as a validity check on the contact. In instances where a non-negative *df/dt* is encountered, the tonal is flagged and no further analysis is performed.

d. Tonal Frequency Range

From the analysis of the power spectrum of background noise and typical airplane passages, it is apparent that the level of background noise is considerably higher at the lower frequencies and falls off rapidly as we progress to the higher frequencies. It is also observed that Doppler shifts are best seen for tonals within the 100 Hz to 2000 Hz frequency range. In the analysis conducted, the search for tonals is limited to above 90 Hz. This is done to exclude possible interfering sources in the low frequency range where the background noise contains a strong, random broadband component which obscures the target. This lower frequency limit can be adjusted by changing the associated parameter in the program.

THIS PAGE INTENTIONALLY LEFT BLANK

IV. DATA ANALYSIS

A. OVERVIEW

Data from a total of ten airplanes (both jet and propellers) were recorded during a one-hour period. The exact time of CPA was recorded manually as the airplane passed overhead. Identification of the target type was based on listening to the air-traffic control radio communications and subsequent verification with airport records (Flightaware, n.d). Post-processing of data included the audio playback of the events, analysis of pressure vs. time (time-domain analysis), and study of the targets' tonals on the LOFARgram (Low Frequency Analysis and Recording gram, i.e., time vs frequency). Table 2 summarizes the target events. This ground-truth forms the basis for evaluating the output results obtained from running the MATLAB program at different threshold settings. Time references to the passage of the airplanes are made in both real time and relative time measured from the start of the recording in seconds.

Time of Event	Relative Time (s)	Type of Target	Airplane ID	Remarks
1021	74	Cessna 182P	N6800M	Single propeller
1031	623	Beech Be30 King Air	N302NC	Twin propellers
1047	1581	Cessna 182	N826DD	Single propeller
1050	1796	Learjet J45	WDR 989	Twin jet
1052	1925	Beech Be9L	N3262R	Twin propellers
1055	2120	Embraer EM120	SKW5558	Twin propellers
1059	2300	Cessna 750 Citation	EJ947	Twin jet
1102	2480	Beech Be 40	OPT 417	Twin jet
1106	2780	Embraer XJ 145	BTA98	Twin jet
1118	3427	Beech Be9L	N6077X	Twin propellers

Table 2. Summary of Recorded Target Events

B. ANALYSIS OF BACKGROUND NOISE

1. Power Spectrum of Background Noise

The background noise level was determined by processing a 300-second recording of the ambient environment noise in the absence of any airplane passage through the relevant functions in MATLAB program 'auto_Doppler_detector.m'. It is observed that the background noise level is highest in the lower frequencies and falls off rapidly as frequency increases. Contributors to this low-frequency noise include, but are not limited to equipment vibration, wind noise, noise from the ocean to the north, vehicles traveling on Highway CA 1 south of NPS, birds, and electronic noise. From the zoom in plot in Figure 14, it is seen that the noise spectrum level decreases most rapidly (-20 dB) in the frequency range between 0 and 200 Hz.

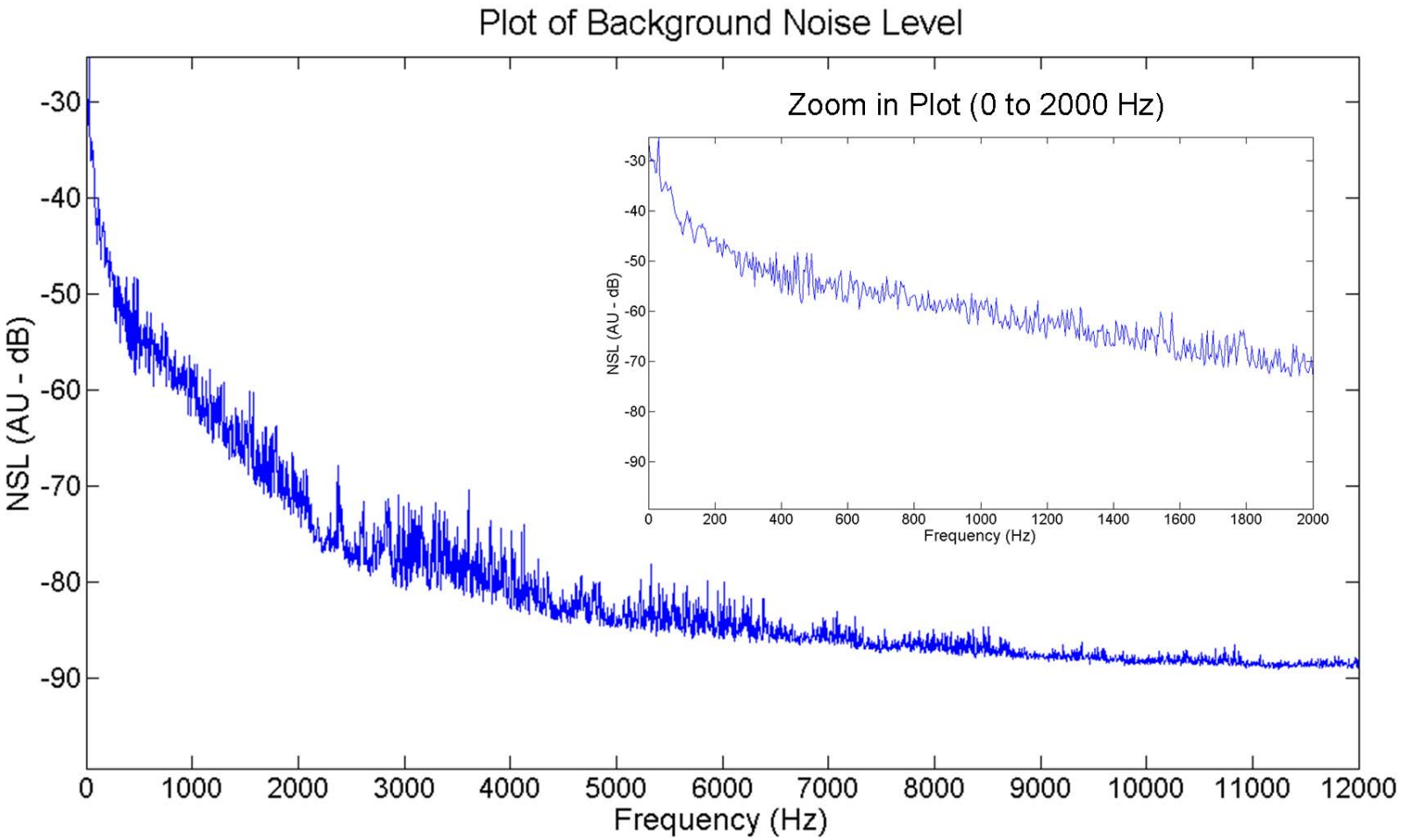

Figure 14. Power Spectrum of Background Noise

2. Threshold Determination

The background noise level is computed to have a mean value of μ=0.0229 and standard deviation of σ=0.0058. These values are expressed in arbitrary units of pressure squared. This mean and standard deviation are used as the baseline for the initial detection threshold. To determine an appropriate cross-correlation, R_{xy} threshold, synthetically generated airplane "events" with various velocities are cross-correlated with the background noise at various time periods and the results averaged. This is repeated for different frequency bands. The mean and standard deviation of the peak of the cross-correlation with noise are designated as μ_r and $\sigma_{r,}$ respectively.

C. ANALYSIS OF DATA – PROPELLER AIRPLANES

Doppler shifts in the 50-1500 Hz region as the airplane passed through CPA are clearly seen for all six propeller airplanes. In most cases, measurements of the upper and lower frequencies of the tonals with good SNR give a good estimate of the velocity through the use of Equation 2.12. Similarly, the rate of change of frequency at CPA is also measured. Processing of the tonals is restricted to those having good SNR at the asymptotes before and after CPA. In one of the cases, there is an observed change in engine revolutions per minute (RPM) just prior CPA, identified by a "knee" in the LOFARgram. The velocity in this case was estimated through measurement of f_0 and f_{Lower} instead.

Program 'auto_Doppler_detector.m' is run with time domain threshold settings of μ+15σ and R_{xy} threshold settings of μ_r+0.5σ_r. A total of 131 peaks (energy exceeding threshold) and 10 airplane contacts with Doppler shifts are detected. A summary of the results obtained with other threshold settings is presented in Section E of this chapter.

1. Event 1 – N6800M at Time 1021 (74s)

N6800M is a four-seat, single-engine CESSNA 182P SKYLANE. Used mainly for training and general aviation, the C182 has a cruise speed of 150 Knots Indicated Airspeed (KIAS) or 75 m/s and a stall speed of 49 KIAS (24.5 m/s). Typical speed during approach for landing is 70 to 80 KIAS (35 to 40 m/s).

	Tonal 1		Tonal 2		Tonal 3		Program
t_0	75 s						74s
	f_{lower}	f_{upper}	f_{lower}	f_{upper}	f_{lower}	f_{upper}	--
	67.14	91.55	97.66	134.3	195.3	274.7	--
Δf	12.21		18.32		39.70		--
f_0	79.35		115.98		235.00		122.07
df/dt	-4.91		-6.46		-15.53		-7.761
v (m/s)	53		54		58		48

Table 3. Observed Parameters of N6800M

There is good correlation between the results obtained by the program and manual analysis.

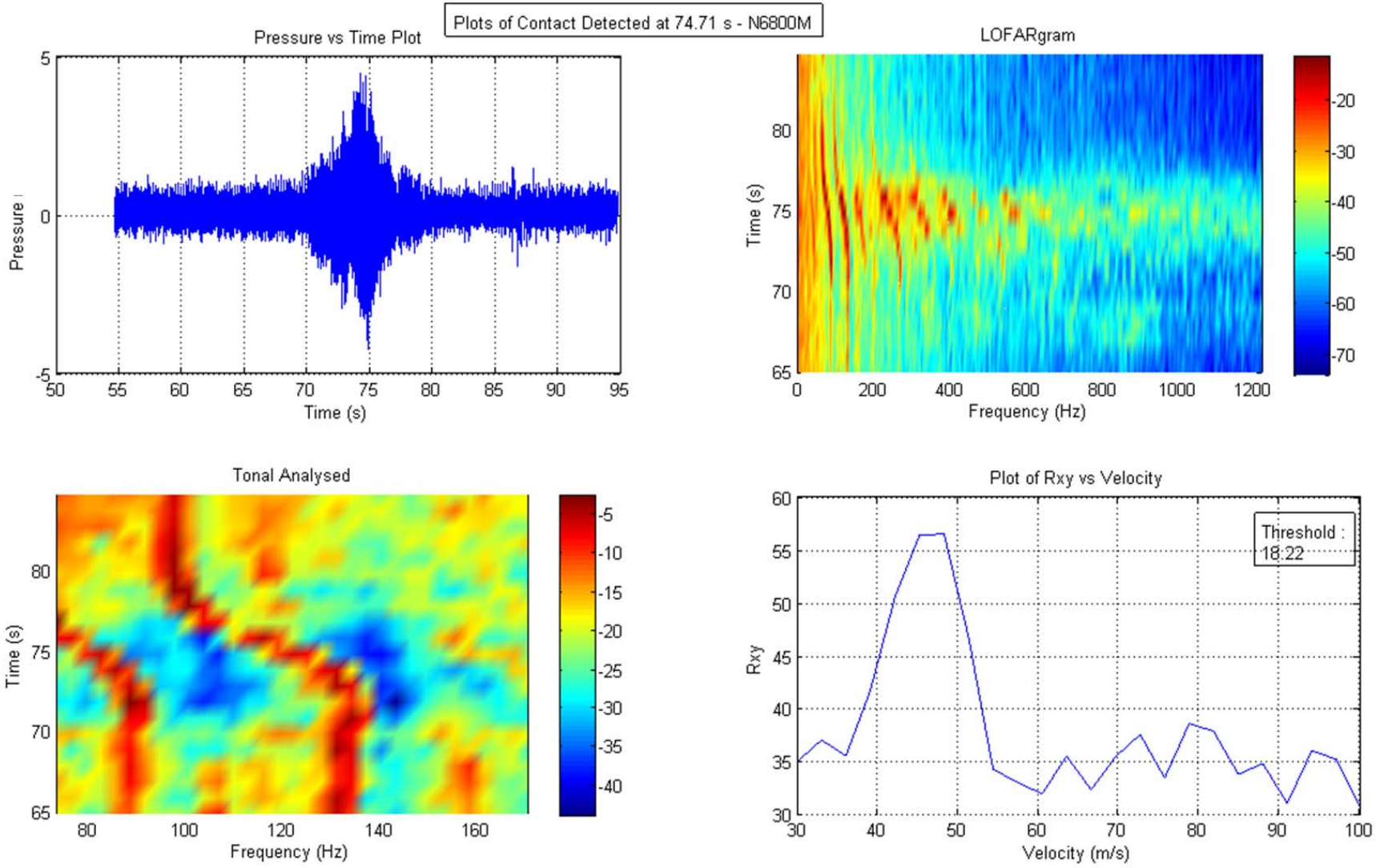

Figure 15. Plot of Results from Analysis of CESSNA 182 SKYLANE, N6800M

2. Event 2 – N302NC at Time 1031 (623s)

The second propeller airplane, N302NC, is a twin-engine, HAWKER BEECH SUPER KING AIR 300 BE30/G. A multi-purpose aircraft, the BE 30 is used for both civil and military purposes. With a cruise speed of 290 KIAS (145 m/s) and a stall speed of 75 KIAS (37.5 m/s), the typical approach speeds is 100 to 120 KIAS (50 to 60 m/s). Only one of the tonals (~ 70Hz) is sharp enough for use in the estimation of Doppler shift. The other tonals at higher frequencies may be "blurred" by both the engines operating at slightly different RPM settings.

	Tonal 1		Program
t_0	623 s		623 s
	f_{lower}	f_{upper}	--
	85.45	122.11	--
Δf	18.33		--
f_0	103.78		94.60
df/dt	-6.35		-4.6566
v (m/s)	61		53

Table 4. Observed Parameters of N302NC

The results obtained by the program agree with those obtained through manual analysis.

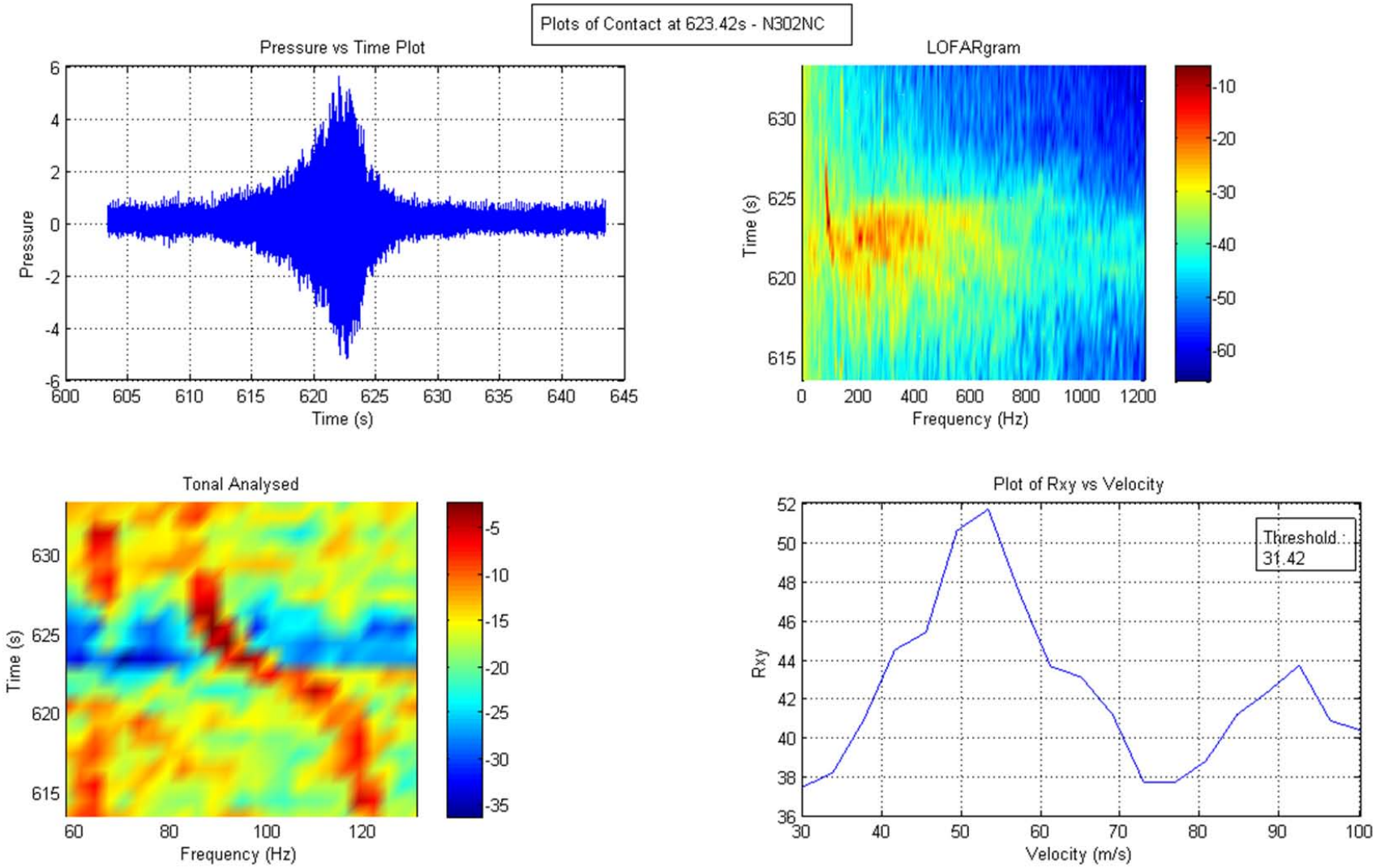

Figure 16. Plot of Results from Analysis of BEECH SUPER KING AIR 300, BE30/G, N302NC

3. Event 3 – N826DD at Time 1047 (1581s)

N826DD is a CESSNA 182T SKYLANE single-engine light airplane similar in performance to N6800M. Multiple tonals with Doppler shifts are observed. Estimation of velocity is obtained with three tonals.

	Tonal 1		Tonal 2		Tonal 3		Program
t_0	1581 s						1582 s
	f_{lower}	f_{upper}	f_{lower}	f_{upper}	f_{lower}	f_{upper}	--
	91.55	128.2	128.2	189.2	213.6	311.3	--
Δf	18.33		30.50		48.85		--
f_0	109.875		158.70		262.45		137.33
df/dt	-6.78		-10.85		-16.37		-9.313
v (m/s)	57		66		64		61

Table 5. Observed Parameters of N826DD

A fourth tonal with f_0 = 855.6Hz is visible. The velocity is estimated to be 61 m/s based on this tonal.

The time of CPA is identified by the program to be later than observed. This is due to the fact that low-frequency noise (marked with an “X” on the LOFARgram) appeared after CPA that skews the total overall energy level.

The estimate of CPA range for this target is 381 m. This is consistent with observations as the airplane was on visual approach to runway 10L.

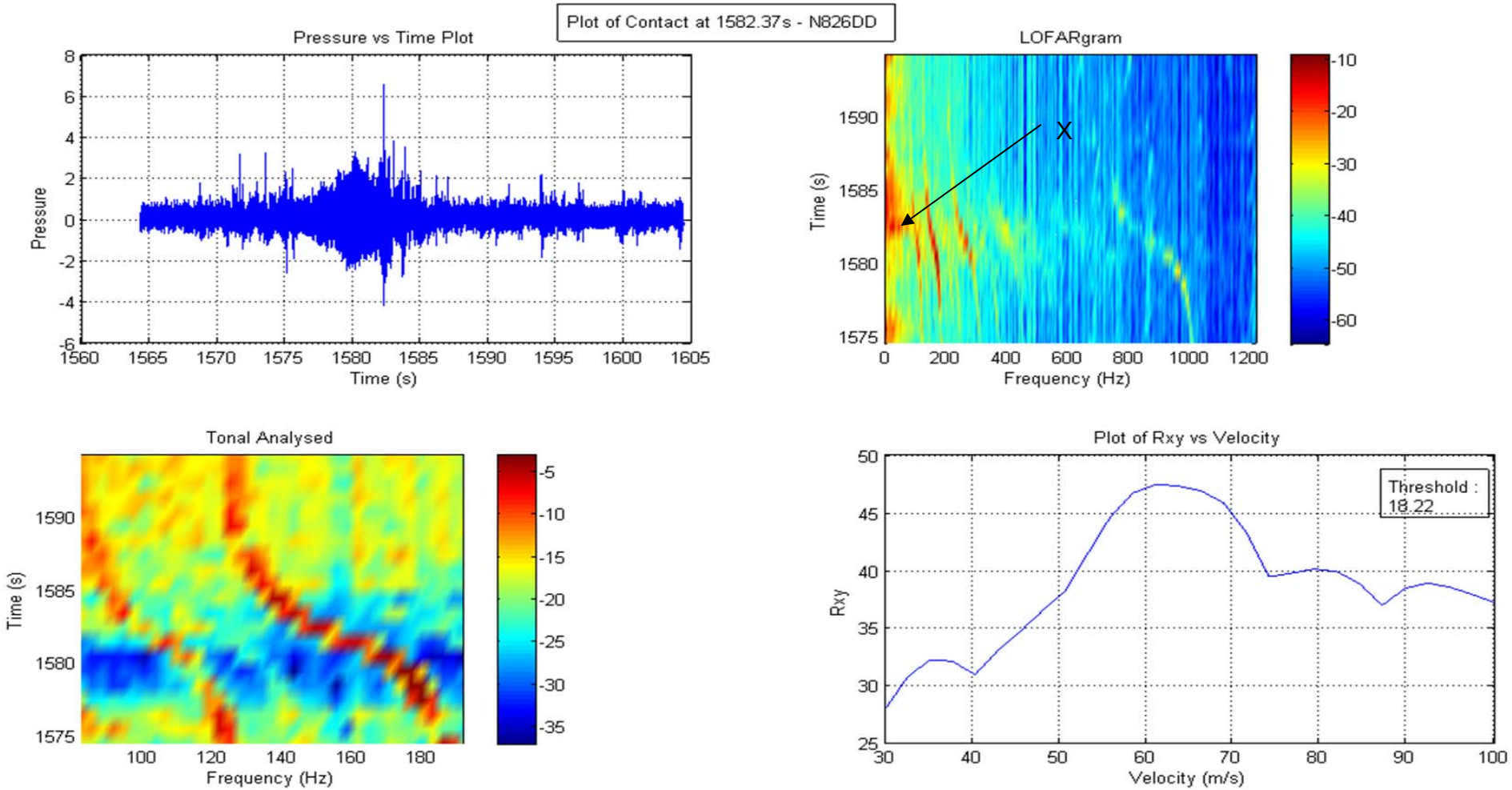

Figure 17. Plot of Results from Analysis of CESSNA 182, N826DD

4. Event 4 – N3262R at Time 1052 (1925s)

N3262R is a twin-engine BEECH KING AIR BE/90. Slightly smaller than the Super King Air 300 in Event 3, the BE/90 is also used extensively by both the military and in civil aviation. With a cruise speed of 260 KIAS (130 m/s) and a stall speed of 78 KIAS (39 m/s), typical approach speed is 100 - 120 KIAS (50 to 60 m/s). Three tonals are observed with only one meeting the required criterion for a good estimation of velocity.

	Tonal 1		Program
t_0	1925 s		1924 s
	f_{lower}	f_{upper}	--
	103.80	158.70	--
Δf	27.45		
f_0	131.25		137.33
df/dt	-16.31		-10.70
v (m/s)	72		48

Table 6. Observed Parameters of N3262R

From the R_{xy} vs. Velocity plot, the velocity 48 m/s has the highest peak and a second velocity peak exist at 77 m/s. This could be due to interference from the noise in the vicinity of t =1930s and a 'line" near 120 Hz between t = 1915s to 1920s (Marked with "X" on plot).

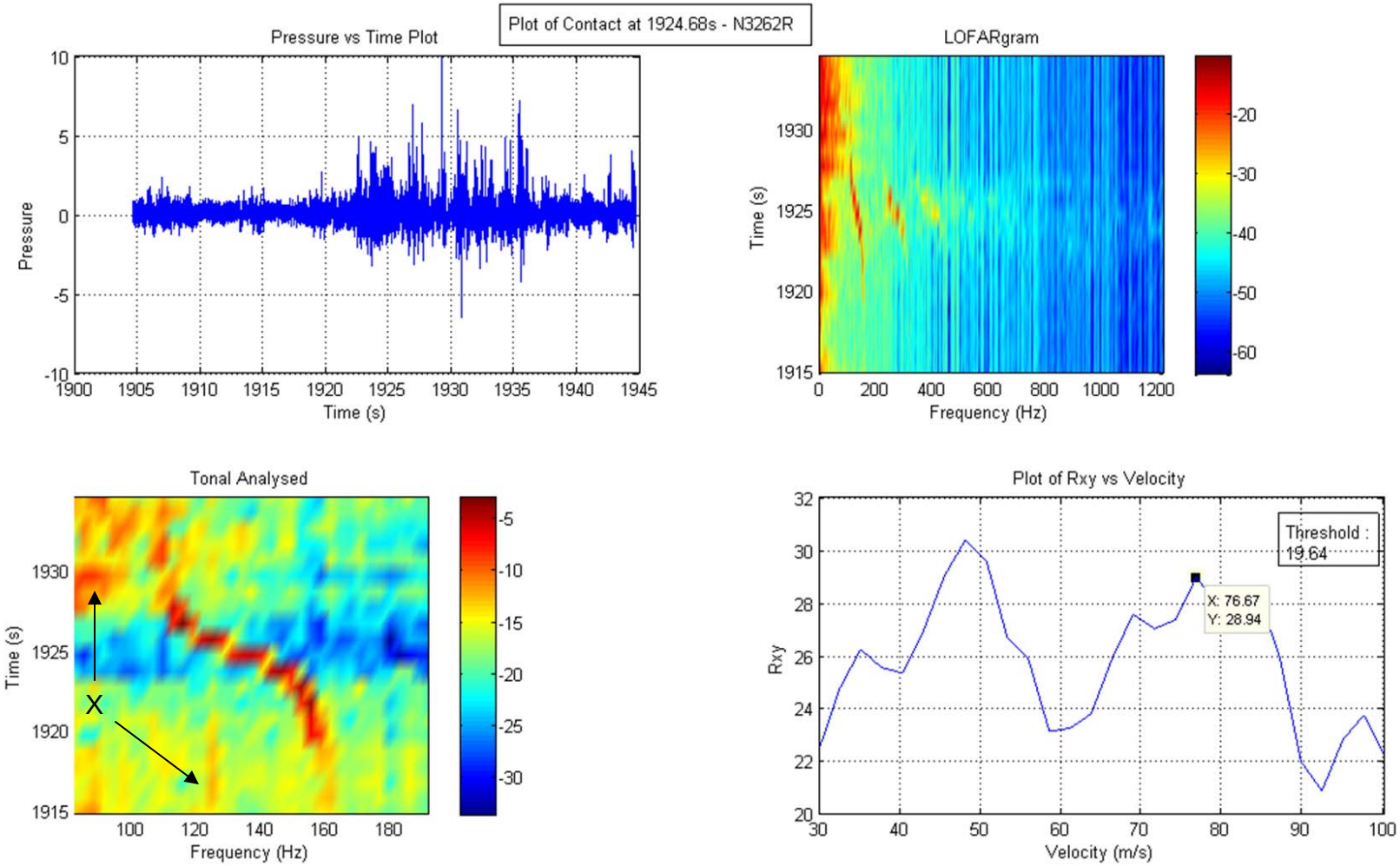

Figure 18. Plot of Results from Analysis of BEECH KING AIR BE90, N3262R

5. Event 5 – SKY5558 at Time 1055 (2120s)

SKYWEST Flight 5558 departed Monterey for San Francisco, flying over the tower at Herrmann Hall at a higher altitude than the other airplanes. The airplane is a twin-engine turboprop Embraer EMB-120 Brasilia. A commuter airplane designed for commercial use, it has a passenger capacity of 30, a cruise speed of 300 KIAS (150 m/s) and a stall speed of 110 KIAS (55 m/s). The airplane was on her climb out during the recording. One tonal line that was clearly distinct and another “half tonal” centred on 240.9 Hz were both used for estimation.

	Tonal 1		Tonal 2		Program
t_0	2121 s				2119 s
	f_{lower}	f_{upper}	f_{lower}	f_{upper}	--
	100.7	143.4	201.1	-	--
Δf	21.35		39.8		--
f_0	122.05		240.9		131.23
df/dt	-6.1833		-10.58		-6.208
v (m/s)	60		57		50

Table 7. Observed Parameters of SKY5558

The results are in agreement with the ground truth. Estimated CPA time is earlier than observed, due in part to the high level of low frequency noise at time 2119s (marked on plot).

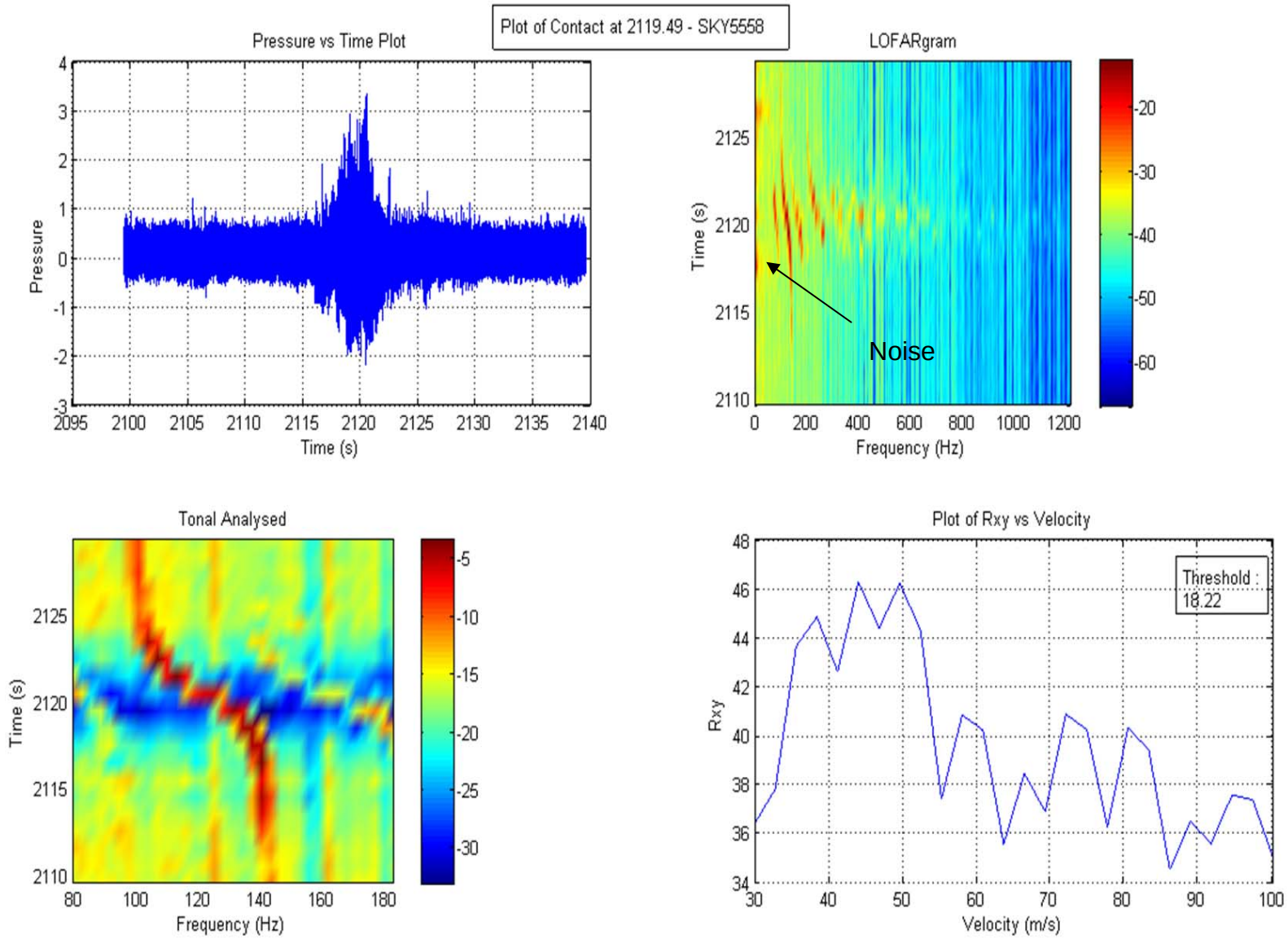

Figure 19. Plot of Results from Analysis of EMBRAER EM120, SKY5558

6. Event 6 – N6077X at Time 1118 (3427s)

The last of the propeller airplanes, N6077X is also a twin-engine BEECH KING AIR 90. There is an observed increase in the engine RPM just before the airplane passes through CPA, which is seen in the shift (knee) in the LOFAR lines. CPA time is estimated from the sound pressure — time plot and the airplane's estimated parameters are as tabulated.

	Tonal 1		Tonal 2		Tonal 3		Program
t_0	3425 s						3425 s
	f_{lower}	f_{upper}	f_{lower}	f_{upper}	f_{lower}	f_{upper}	--
	140.4	-	152.6	-	225.8	-	--
Δf	24.40		36.60		55.00		--
f_0	140.40		189.20		280.80		283.81
df/dt	-5.43		-5.78		-16.27		-6.208
v (m/s)	60		66		67		30

Table 8. Observed Parameters of N6077X

Although the passage is correctly identified by the program, the R_{xy} value is barely above threshold. The change just prior to CPA and the resulting absence of a complete Doppler shift gives a poor estimate of *df/dt* and velocity.

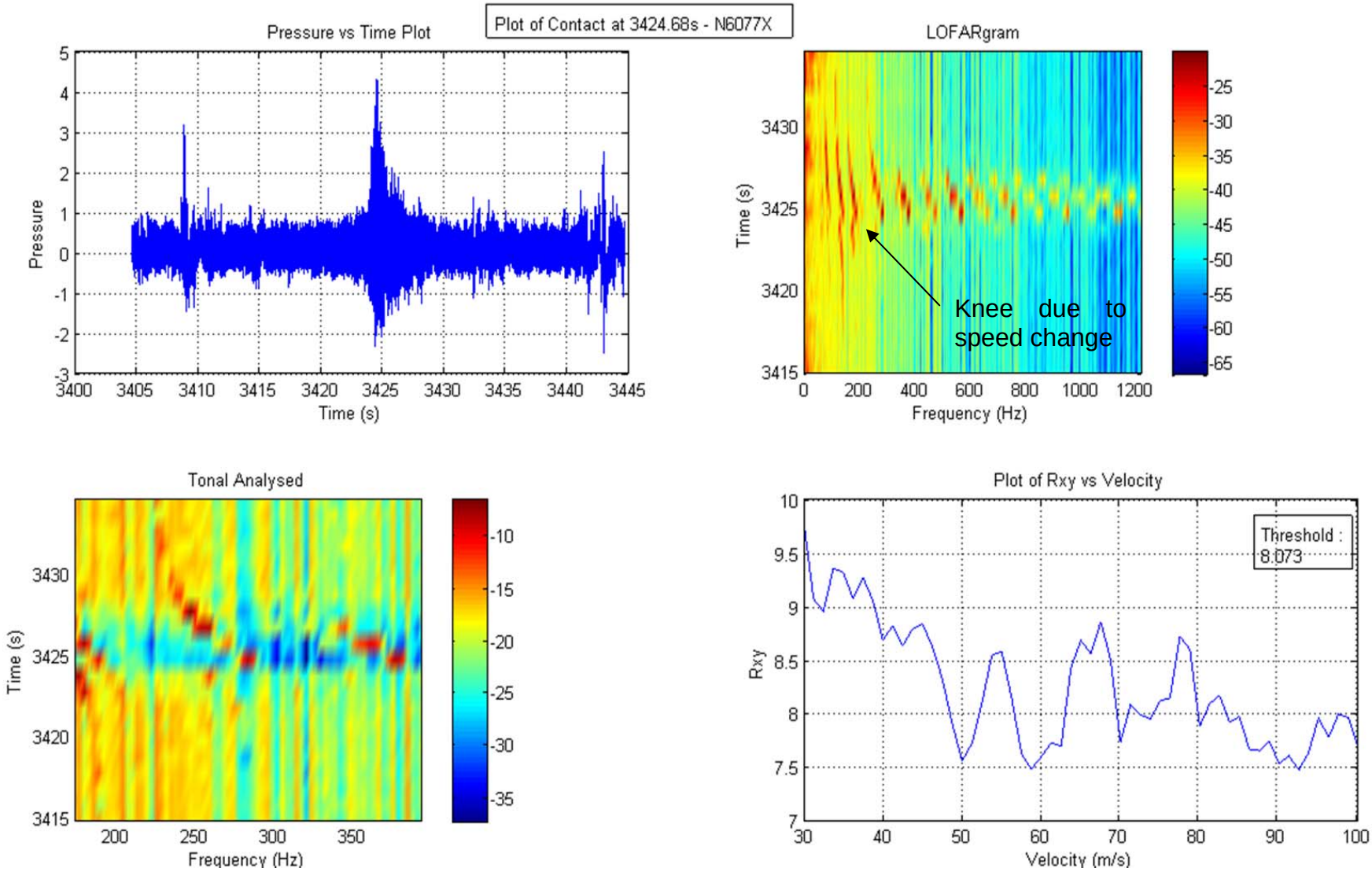

Figure 20. Plot of Results from Analysis of BEECH KING AIR BE 9L, N6077X

D. ANALYSIS OF DATA – JET AIRPLANES

The LOFARgrams of the jet airplanes are observed to be broadband with energy extending into the 12 kiloHertz (kHz) region. While the targets are detected as “peaks” in the time domain, there are however no distinct tonals that can be tracked. The Doppler shift patterns that are visibly observable for the propeller airplanes are absent here.

A total of four jet airplanes are recorded. All of them have twin engines and cruise speeds of 450 to 600 KIAS (225 to 300 m/s). Approach speed is typically 150 to 200 KIAS (75 to 100 m/s) for these airplanes, which is considerably higher than the propeller airplanes.

1. Event 7: LEARJET J45 (WDR989) at Time 1050 (1796s)

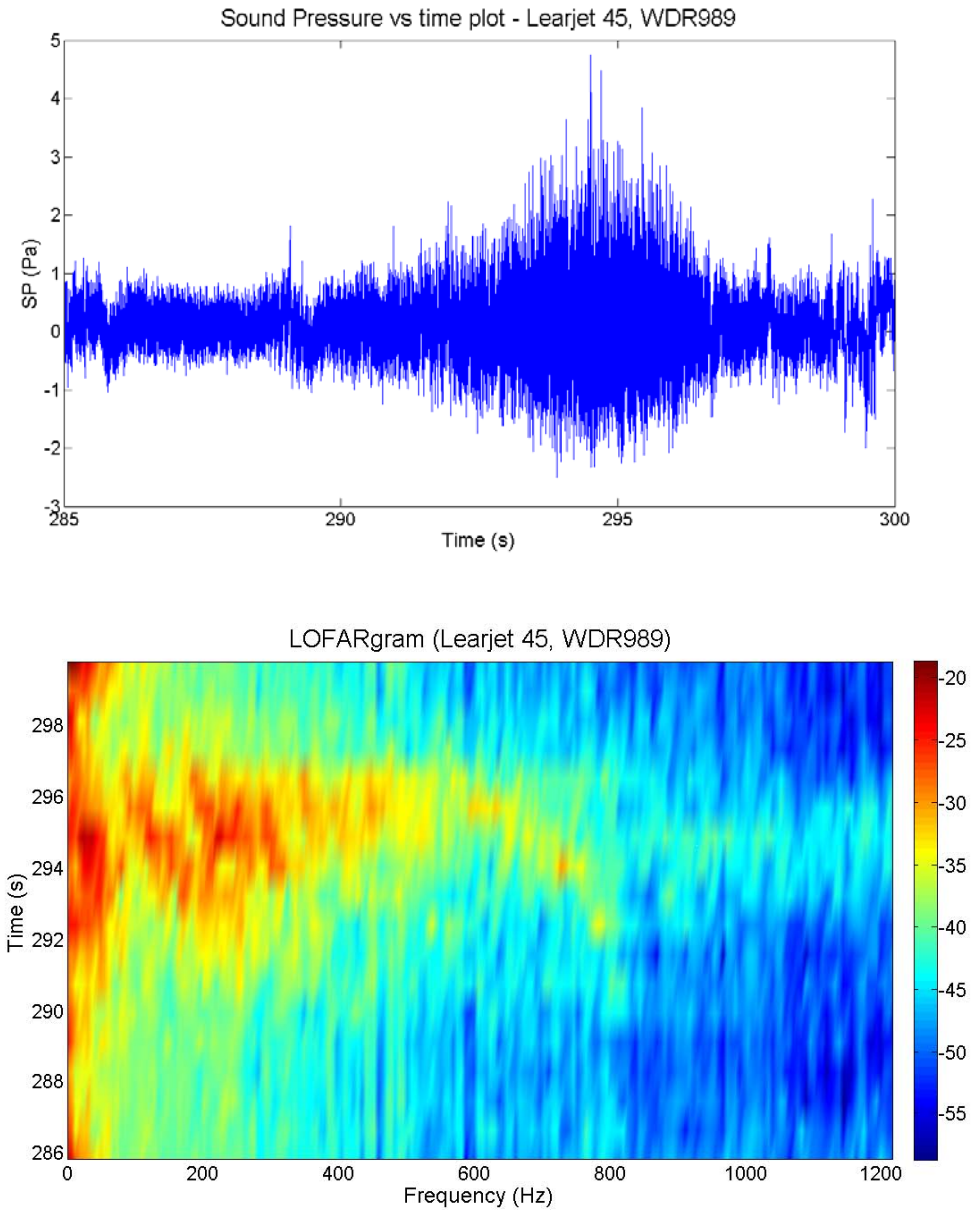

Figure 21. Pressure vs. Time Plot and LOFARgram of LEARJET J45, WDR989

2. Event 8: CESSNA Citation C750 (EJ 947) at Time 1050 (1796s)

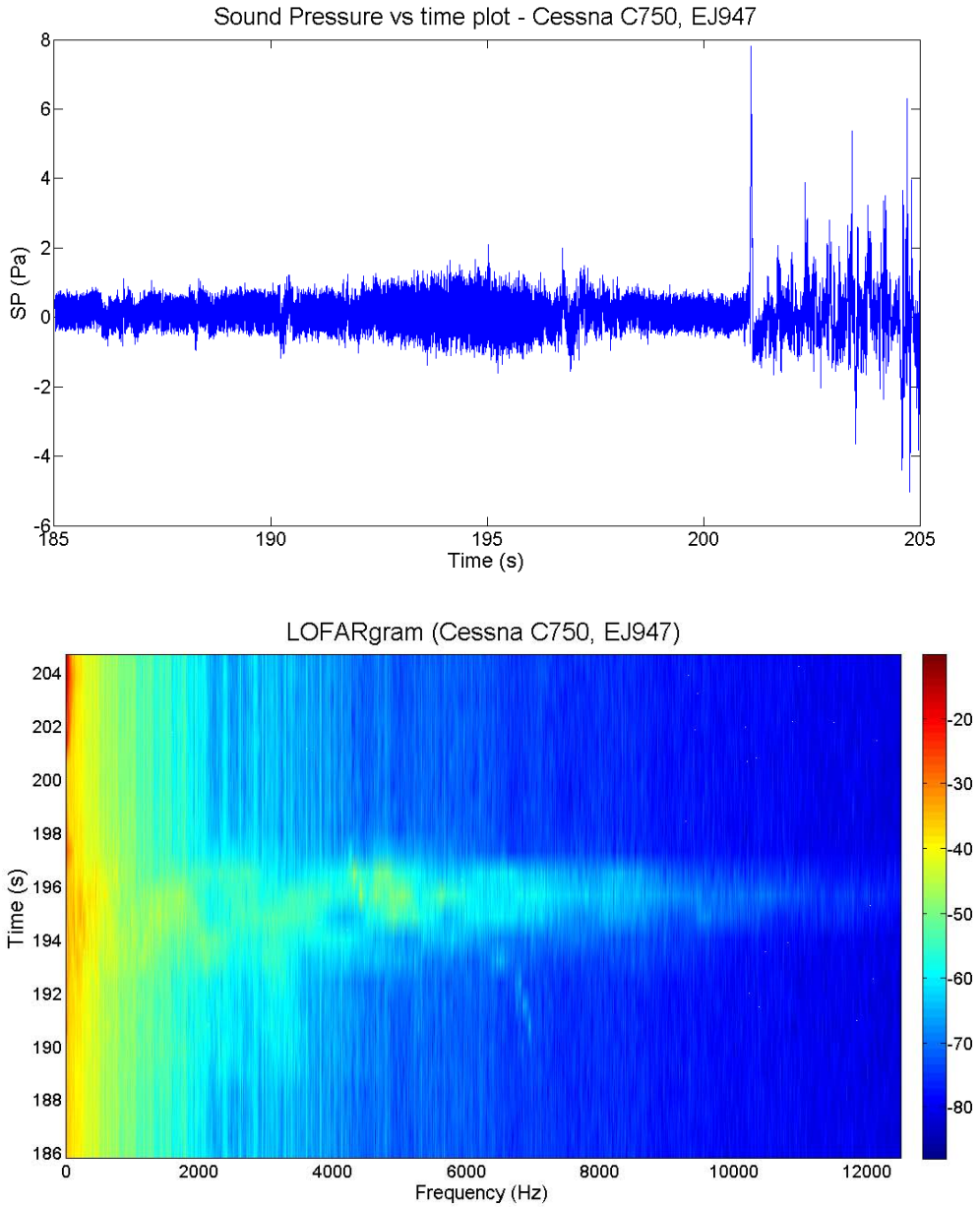

Figure 22. Pressure vs. Time Plot and LOFARgram of CESSNA C750, EJ947

3. Event 9: BEECH Be40 (OPT417) at Time 1102 (2480s)

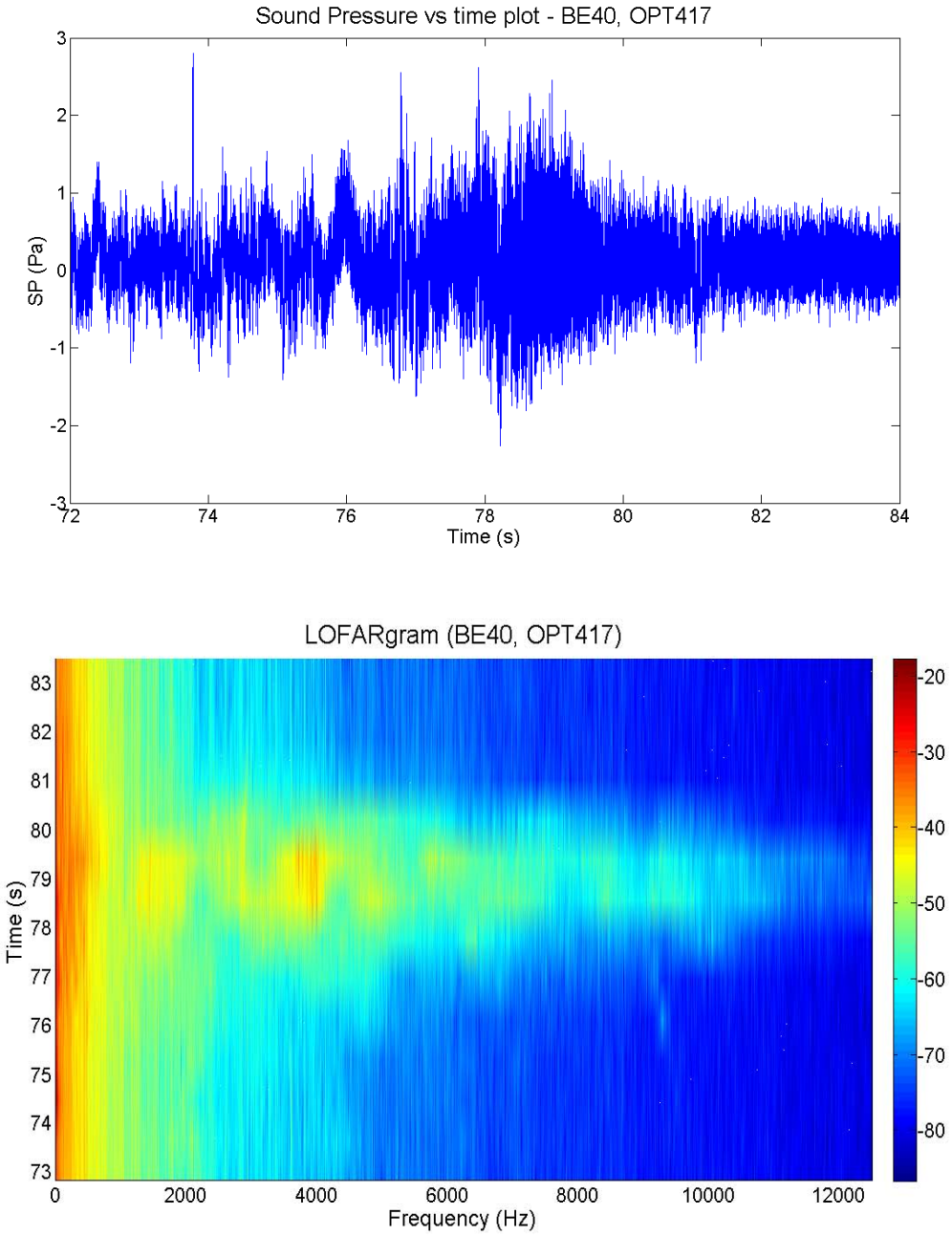

Figure 23. Pressure vs. Time Plot and LOFARgram of BEECH Be40, OPT417

4. Event 10: EMBRAER XJ 145 (BTA98) at Time 1106 (3427s)

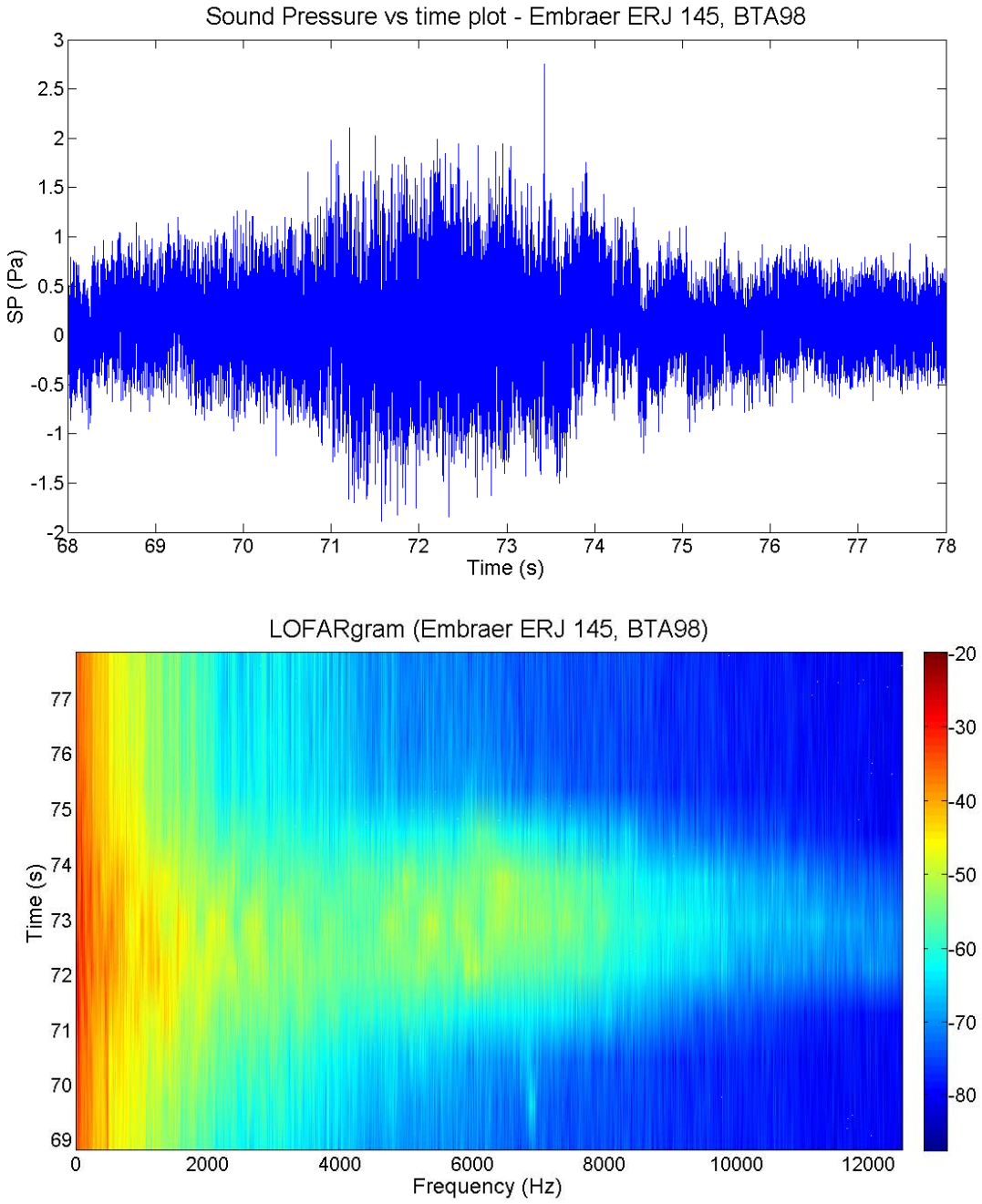

Figure 24. Pressure vs. Time Plot and LOFARgram of EMBRAER ERJ 145, BTA98

E. PERFORMANCE OF THE AUTO-DETECTION PROGRAM

Using the threshold settings $\mu+15\sigma$ and R_{xy} threshold setting of $\mu_r+0.5\sigma_r$, the algorithm successfully identified all six propeller airplanes. Of the 10 "detected with Doppler calls," there were four instances of false alarm.

The processing is repeated with other combinations of threshold settings of $\mu+T\sigma$ and R_{xy} threshold setting of $\mu_r+R\sigma_r$. The results are tabulated below. The output analysis reports are included in Appendix H. It is seen that the energy threshold setting affects mainly the number of peaks detected while the R_{xy} threshold setting affects mainly the number of Doppler shifts observed. Above a certain threshold setting, however, the propeller planes are "cut off" and the number of correct detections falls off.

Run	Threshold Setting, T	R_{xy} threshold setting, R	No. of Peak	No. of Doppler	Remarks
1	15	0.5	131	10	4 false contacts
2	15	1.0	131	5	N6077X not detected
3	20	0.5	113	7	2 false contacts
4	20	1.0	113	5	N6077X not detected
5	48	1.0	65	5(4)	Only 4 airplanes detected. 1 double-count

Table 9. Summary of Results using auto_Doppler_detector.m

It is clear from the results that the correct identification of the CPA time t_0 impacts the results significantly. In Events 1 and 2, t_0 determined by the algorithm is close to the observed CPA time and the estimates of velocity and range are close to the ground truth. In addition, the R_{xy} is significantly larger than the threshold value and the R_{xy} -velocity curve has a sharp peak with steep sides. In Event 3, we see the "rounding" off of the peak as CPA time starts to deviate from observed.

As the experiment was conducted using targets of opportunity rather than controlled contacts with known velocity and passing distance, an accurate assessment of the algorithm's performance and accuracy cannot be made. However, the velocities obtained are all within typical velocities for the respective types of airplanes on approach to landing.

As observed in the various LOFARgrams of jet airplanes, the signals are broadband and spread over a wider range of frequencies than the propeller planes. The absence of distinct tonals enables the algorithm to correctly discriminate between these targets and the propeller planes using the Doppler filter.

F. CONCLUSION

The experimental results show that using the presence or absence of the Doppler shift enables selection of a low threshold for energy detection without concern that the detector will be overwhelmed by false alarms. The number of initial detections using energy criterion is filtered down to a manageable number by the secondary criterion involving Doppler.

It is seen that the Doppler shift pattern is useful in two main ways. First, even when the threshold for energy detection is set at a relatively low level, the use of a "second level filter" significantly reduces the number of contacts that have to be analysed by automatically filtering out those that do not meet the defined criteria. This reduces P_{fa} when a false alarm is taken to be a

misidentification as well as a “mis-detection.” Finally, valuable information (velocity and CPA range) is also derived automatically although these estimates may be limited in accuracy.

THIS PAGE INTENTIONALLY LEFT BLANK

V. CONCLUSION AND RECOMMENDATIONS FOR FUTURE DEVELOPMENTS

A. ACCURACY OF RESULTS

The use of the Doppler shift in the decision process has been shown to improve the performance of an automatic detector for a target passing through CPA compared to detection based solely on energy levels. Doppler shift as an additional criterion allows the threshold to be set near the noise floor while achieving a lower P_{fa}. The performance of the detector in the estimation of contact velocity and range relies on the following factors.

1. Determination of CPA Time

The time of CPA is the basis for the analysis of the Doppler pattern. In our study, the CPA time is based on the assumption that the total energy in the frequency domain peaks during CPA. This is subject to two possible ways in which errors affecting the results can be introduced.

First, the Doppler-Range (frequency–time) ambiguity due to the Fourier transform process places a limitation on the time resolution that can be obtained for a specific desired frequency resolution. The CPA time that is determined within the frequency domain is hence an indication that CPA is happening sometime within a time block rather than at a specific resolved time. Depending on the speed and CPA range, this could translate to significant distance between the measured and actual CPA. Secondly, the possibility of interfering contacts or background noise occurring in the vicinity of CPA time can displace the peak and hence affect the accuracy of the results.

While the latter is due to factors that are beyond control, improvements can be made to mitigate the effect of the former. Determining the CPA time in the time domain by tracking the trend of the magnitude of the received signal and tagging CPA to the maximum will allow CPA time to be declared with a better

resolution. Alternatively, since it is the total energy across all frequencies, the power spectral density could be calculated with a short integration time, sacrificing frequency resolution, purely to estimate the CPA time. Finally, if the sensor has other information (e.g., contact bearings), these could be used to refine the CPA time.

2. Measuring the Rate of Frequency Change, *df/dt*

The rate of frequency change, *df/dt* is one of the two parameters that generates the template Doppler curves used in the cross-correlation with the measured signal. Once determined, this is not varied. Only the velocity is varied in the cross-correlation process. The *df/dt* is estimated based on the assumption that in the time blocks before and after CPA, the strongest frequency corresponds to that of f_0. This again could be subject to errors from interfering noise sources. In addition, the number of differences that could be used in determining *df/dt* is constrained by the need to limit the analysis to the vicinity of CPA to ensure that the assumption in Eq. 2.8 holds. This, in turn, is determined by the passing range and the velocity of the contact. A fast contact at close range means that the contact is within the acceptable range of values near CPA for only a very short period of time and the number of points used to determine *df/dt* is small.

An improvement might involve the use of cross-correlation to determine *df/dt* instead. Lines of different slopes could be correlated to the measured signal for the best estimation of *df/dt*.

3. Number of Tonals

Our analysis only involves the use of a single tonal even in cases where there are several tonals that exhibited good SNR for analysis. A more accurate estimate could be obtained if more tonals are used. The results from reading several *df/dt* values could be plotted against their corresponding f_0 values and the

slope obtained with linear regression could be used to provide a better estimate of $\frac{v^2}{R_o}$.

B. CONCLUSION

The objectives set forth for this thesis have been met. It has been demonstrated with one hour of recording that the Doppler effect can be used to improve the passive automated detection of contacts. The estimates of velocity and range for the airplanes are within expectations based on ground-truth observations. Finally, the detection algorithm developed here is compact and could realistically be deployed in acoustic sensors as part of an underwater surveillance network.

C. RECOMMENDATIONS FOR FUTURE DEVELOPMENT

It is recommended that steps to improve the determination of CPA time and *df/dt* be explored in the future. Improvements in the estimate of these parameters will improve the overall detection performance in terms of P_d and P_{fa}. In addition, the current detection algorithm could be extended to use more than one tonal.

Another follow-up step is to extend the detection algorithm to the determination of contacts in an underwater environment. This extension will be complicated by the complexity of underwater acoustics, including multipath propagation, refraction, and noise variability. However, underwater detection will be aided by the slower target speeds and longer integration times.

THIS PAGE INTENTIONALLY LEFT BLANK

APPENDIX A. TECHNICAL SPECIFICATIONS

A. Technical Specifications for Data Acquisition Module

USB Dynamic Signal Acquisition

NI USB-9233

- 24-bit resolution
- 102 dB dynamic range
- 50 kS/s max rate per channel
- 4 simultaneous analog inputs
- ±5 V input range
- AC coupled with IEPE power
- Hi-Speed USB 2.0

Recommended Software

- LabVIEW
- LabVIEW Sound and Vibration Toolkit
- LabVIEW Order Analysis Toolkit
- LabWindows/CVI
- Measurement Studio
- DAQmx

Overview

The National Instruments USB-9233 is a four-channel dynamic signal acquisition module for making high-accuracy measurements from IEPE sensors. The NI USB-9233 delivers 102 dB of dynamic range and incorporates IEPE signal conditioning for accelerometers and microphones. The four USB-9233 input channels simultaneously acquire at rates from 2 to 50 kHz. In addition, the module includes built-in antialiasing filters that automatically adjust to your sampling rate.

Hardware

Data rates on the four simultaneous input channels of the USB-9233 range from 2 to 50 kHz. Each signal is AC coupled, buffered, analog prefiltered, and sampled by a 24-bit delta-sigma analog-to-digital converter (ADC) that performs digital filtering with a cutoff frequency that automatically adjusts to your data rate. The USB-9233 module features a voltage range of ±5 V and a dynamic range of over 100 dB. Communication to the USB-9233 is Hi-Speed USB 2.0, guaranteeing data throughput.

The USB-9233 is a nonisolated module that provides ±30 V of overvoltage protection (with respect to chassis ground) for IEPE sensor connections. IEPE excitation and AC coupling are not software-selectable and are always enabled.

The USB-9233 uses a method of A/D conversion known as delta-sigma modulation. If the data rate is 25 kS/s, each ADC actually samples its input signal at 3.2 MS/s (128 times the data rate) and produces samples that are applied to a digital filter. This filter then expands the data to 24 bits, rejects signal components greater than 12.5 kHz (the Nyquist frequency), and then digitally resamples the data at the chosen data rate of 25 kS/s. This combination of analog and digital filtering provides an accurate representation of desirable signals while rejecting out-of-band signals. The built-in filters automatically adjust themselves to discriminate between signals based on the frequency range, or bandwidth, of the signal.

Software

The USB-9233 uses NI-DAQmx as the hardware and OS interface, so you can build automated test systems or integrate the USB-9233 with other hardware, including National Instruments multifunction DAQ products and CAN devices, through NI-DAQmx function calls for NI LabVIEW, LabWindows/CVI, and Measurement Studio.

Other useful NI-DAQ driver software features include:

- Automatic Code Generation – DAQ Assistant is an interactive guide that steps you through configuring, testing, and programming measurement tasks and automatically generates the necessary code for LabVIEW, LabWindows/CVI, or Measurement Studio.
- Test Panels – With NI-DAQ, you can test all of your device functionality before you begin application development.
- LabVIEW Integration – All NI-DAQ functions use the waveform data type, which carries acquired data and timing information directly into more than 400 LabVIEW built-in analysis routines for display of results in engineering units on a graph.

Analysis Software

Because of its bandwidth, the USB-9233 is well-suited for applications in noise and vibration analysis. These applications are specifically addressed in the LabVIEW Sound and Vibration and LabVIEW Order Analysis toolkits. By using these toolkits in conjunction with a USB-9233 module, you can produce power spectra, frequency responses, fractional-octave analysis, sound-level measurements, order spectra, order maps, order extraction, and sensor calibration. The USB-9233 is ideal for a wide variety of mobile/portable applications such as industrial machine condition monitoring and in-vehicle noise, vibration, and harshness testing

NATIONAL INSTRUMENTS

(From: National Instruments, n.d.)

Specifications

The following specifications are typical for the range 0 to 60 °C unless otherwise noted.

Input Characteristics

Number of channels ..... 4 analog input channels
ADC resolution ..... 24 bits
Type of ADC ..... Delta-sigma (with analog prefiltering)

Data rate (fs)
- Minimum ..... 2 kS/s
- Maximum ..... 50 kS/s

Master timebase (internal)
- Frequency ..... 12.8 MHz
- Accuracy ..... ±100 ppm max

Input coupling ..... AC

AC cutoff frequency
- -3 dB ..... 0.5 Hz typ
- -0.1 dB ..... 4.2 Hz max

AC voltage full-scale range
- Typical ..... 5.4 V_{peak}
- Minimum ..... 5 V_{peak}
- Maximum ..... 5.8 V_{peak}

Common-mode voltage (AI- to earth ground) ..... ±2 V

IEPE excitation current
- Minimum ..... 2.0 mA
- Typical ..... 2.2 mA

IEPE compliance voltage ..... 19 V max

Overvoltage protection (with respect to chassis ground)
- For an IEPE sensor connected to AI+ and AI- ..... ±30 V
- For a low-impedance source connected to AI+ and AI- ..... -6 to 30 V

Input delay (in seconds)
- ≤ 25 kS/s ..... 12.8 / fs
- > 25 kS/s ..... 9.8 / fs

Accuracy (0 to 60 °C)

Error	Accuracy
Calibrated max	±0.3 dB
Calibrated typ	±0.1 dB
Uncalibrated max	±0.6 dB

Accuracy drift
- Typical ..... 0.001 dB/°C
- Maximum ..... 0.0045 dB/°C

Channel-to-channel matching
- Gain
  - Maximum ..... 0.27 dB
  - Typical ..... 0.07 dB
- Phase (*fin* in kHz) ..... *fin* · 0.077° + 0.067°

Dynamic characteristics

fs	Passband			
	Freq	Flatness (pk-to-pk max)	Freq	Phase Nonlinearity
≤25 kS/s	0.45 · *fs*	0.05 dB	0.45 · *fs*	±3.4°
>25 kS/s	0.42 · *fs*	0.05 dB	0.41 · *fs*	±1.3°

fs	Stopband		Oversample Rate	Alias-Free Bandwidth
	Freq	Attenuation		
≤25 kS/s	0.58 · *fs*	95 dB	128 · *fs*	0.42 · *fs*
>25 kS/s	0.68 · *fs*	92 dB	64 · *fs*	0.32 · *fs*

Crosstalk
- Paired channels (0 and 1, 2 and 3) ..... -100 dB at 1 kHz
- Nonpaired channels ..... -110 dB at 1 kHz

Common-mode rejection ratio (CMRR)
- Minimum ..... 54 dB, *fin* ≤ 1 kHz
- Typical ..... 80 dB, *fin* ≤ 1 kHz

Spurious-free dynamic range (SFDR) ..... 120 dB (*fin* = 1 kHz, -60 dB FS)

Idle channel noise and noise density

Idle Channel	50 kS/s	25 kS/s	2 kS/s
Noise	95 dB FS	98 dB FS	102 dB FS
Noise density	400 nV/√Hz	400 nV/√Hz	900 nV/√Hz

Input impedance
- Differential (AC) ..... >300 kΩ
- AI– (shield) to chassis ground ..... 50 Ω

Distortion
- Harmonic (THD)

	1 kHz, -40 to 70 °C	10 kHz, 25 to 70 °C	10 kHz, -40 to 25 °C
-1 dB FS	-90 dB	-80 dB	
-20 dB FS	-95 dB	-90 dB	-80 dB

- Intermodulation (full-scale input)
  - DIN 250 Hz/8 kHz
    - 4:1 amplitude ratio ..... -80 dB
  - CCIF 11 kHz/12 kHz
    - 1:1 amplitude ratio ..... -93 dB

(From: National Instruments, n.d.)

B. Technical specifications of ACO Pacific Microphone

1. Cartridge model 7046

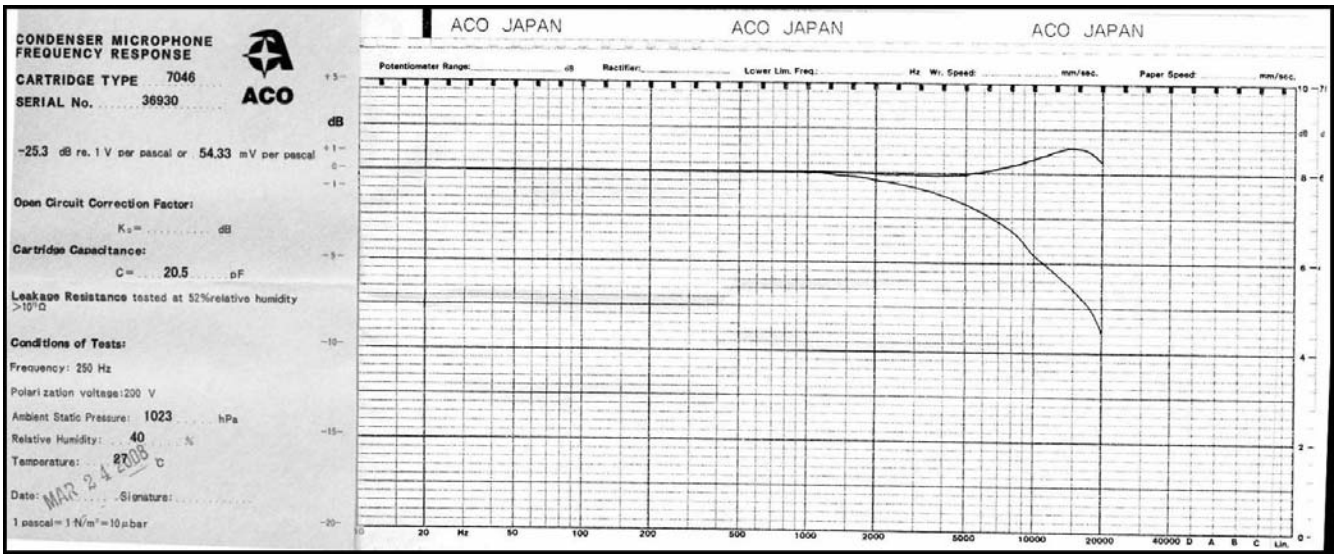

2. 4012 – 1/2 Inch Preamplifier (From: Aco Pacific, n.d.)

Specifications

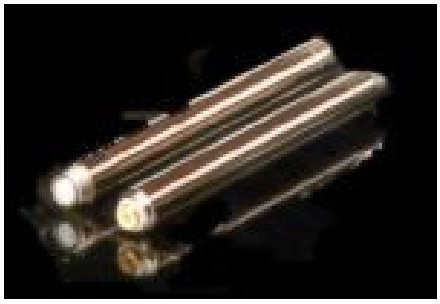

1. 28 Vdc, 22 pF (DM2-22 Dummy Mic) Terminated
2. Frequency Response:
   <2 Hz to >200 kHz +/- 0.5 dB,
   0.5 Hz to >> 200 kHz +/- 2 dB
3. Insertion Loss: <<0.25 dB @ 1 kHz
4. Noise:
   "A" Weighted - <1.2 uV typ.
   Linear 20 to 20 kHz - 3 uV
5. Input Impedance: >50 G//0.1 pF
6. Output Voltage: >7 Vrms @28 Vdc Typical
   >15 Vrms @50 Vdc
7. Power Requirements:
   28 Vdc @ <1 mA (HP option <2 mA)
   50 Vdc @ <2 mA (HP option <4 mA)

THIS PAGE INTENTIONALLY LEFT BLANK

APPENDIX B. MATLAB CODE : AUTO_DOPPLER_DETECTOR.M

```
%  Auto Doppler Detector Program.

%  Purpose : This program search a time domain input signal for Doppler
%  Shifts and computes the velocity and passing range of the contact.
%  Detection is based on user determined threshold.

%  Input :  07_aug_08.txt   :  Input time domain data file
%         threshold.mat   :  threshold data generated using
%                         'generate_threshold.m'

%  Output:  07_aug_08_result.txt :  Tabulated time, frequency, velocity %
                    and range results from analysis.
%         Various plots of detected peaks with Doppler Shift.

%  Variables  :
%
%   infile, outfile           :   File names of input and output file.
%   Fs                        :  Sampling frequency derieved from input data.
%   time_length (s)           :  User specified length of data to process in each
%                              cycle.  Recommended to note MATLAB limitations
%                              of array size.
%   time_duration (s)         :  User specified expected total duration of each
%                                passage.
%   input                     :  Time domain signal data read from infile.
%   y                         :  input data tagged with time of data information.
%   del_f,int_t               :  frequency resolution desired and integration
%                               time for computation of power spectral.
%  threshold_setting,Rxy_threshold  :  User specified threshold.

%  Functions called :      time_to_freq.m
%                          find_peak.m,
%                          calc_df_dt.m
%                          peak_compare.m,
%                          generate_template.m (used by function peak_compare.m)
%
%  Comments  :  Input text file is generated using NATIONAL LAB LABVIEW
%                  Express software, converted from .tdms to .txt.  The
%                  first 7 lines contains setting information related to
%                  the recording and data starts on the 8th line.

%                  :  Desired threshold is through the setting of variable
%                  "threshold_setting".  This adds the mean threshold the
%                  corresponding number of 'Standard Deviation'.

%                  :  Output file name is tagged to input file name.  the suffix '_results' is added.

%  Written by How Whye Keong, NPS, 05 Jan 2009

%%%%%%%%%%%%%%%%%%%%%%%%%%%%%%%%%%%%%%%%%%%%%%%%%%%%%%%%%%%%%%%%%%%%%%%%%%%
```

```
close all
clear all;

%%%  Setting of Variables  %%%
infile='07_aug_08.txt';              % Name of input file

time_length     = 300;               %  length of each segment to be read in sec.
time_duration   = 20;                %  length of the expected passage of interest

del_f = 4;                           %  Desired freq resolution.
int_t = 1;                           %  Integration time
threshold_setting = 20;              %  Desired thershold setting.
Rxy_threshold = 0.5;                 %  Desired Rxy threshold setting.


fid=fopen(infile,'r');               % Open file for reading only

line1 = fgetl(fid);                  % Reads line 1 as character string
line2 = fgetl(fid);                  % Reads line 2 as character string
line3 = fgetl(fid);                  % Reads line 3 as character string
line4 = fgetl(fid);                  % Reads line 4 as character string
line5 = fgetl(fid);                  % Reads line 5 as character string
line6 = fgetl(fid);                  % Reads line 6 as character string
line7 = fgetl(fid);                  % Reads line 7 as character string

start_time=line4(1:20);
delta_time=line6(1:8);
delta_time = str2double(delta_time);

Fs = round(1/delta_time);            % Sampling Frequency.  Round to ensure integer

clear line1 line2 line3 line4 line5 line6 line7;

%  Read the stipulated data from input file and tag the corresponding
%  real time to data points.

%  The output is matrix y of sound pressure of time_length with padding
%  of buffer_length to the begining and end.  Exception is the first
%  segment.

time_tracker = 0;                    %  Initialise time_tracker, peak_count &
peak_count = 0;                      %  detection_count.
detection_count=0;

time_duration = floor(time_duration/2);

for j = 1 : 100

%%%%  Read data from file %%%%%%%%%%%%%%%%%%%%%%%%%%%%%%%%%%%%%%%%%%%%%%%
```

```
%  Determine number of data points to read
  if j == 1
     data_pts=  (time_length + time_duration) * Fs;
  else
     data_pts=  time_length * Fs;
  end

  disp(' ');
  disp('Loading data ...');
  input = fscanf(fid,'%f\n',[1,data_pts])';              % Reads data from file

  if isempty(input)
     disp('End of file reached.');
     break;
  else
     %  Create real time vector (Required for plotting)
     time_vec = linspace(1, length(input),length(input))';
     time_vec = (time_vec - 1) * delta_time;
     time_vec = time_vec + time_tracker;

     time_tracker = (j* time_length) + time_duration;

     y = [ time_vec  input];

    %  Store the last segment of data to be attached to the next
          %  data segment read.
    if j == 1
      y_buffer_before = y(((time_length - time_duration)*Fs)+1 : ...
                                        length(input) , :);
     else
      y = [y_buffer_before ; y];

      m = size(y);
      y_buffer_before = y ((m(1)-(2*time_duration*Fs))+1 : m(1), :);
    end
  end

  disp(['Data from segment ',num2str(j),' loaded...']);


  %%%  Convert to Frequency domain and locate energy peaks %%%

  %  Performs FFT on input signal

  disp ('Performing FFT...');

  [f,t,lofar] = time_to_freq(y(:,2),Fs,del_f,int_t);
  t = t + y(1,1); %  Align time vector of LOFARGRAM to real time
  disp ('FFT completed');
```

```
%%% Locate the instances where energy is above threshold %%%

   % Load threshold data.

   if j==1
     load threshold.mat;
     threshold = threshold + threshold_setting*SD;  %  Set threshold
     threshold_vec(4,:) = threshold_vec(2,:) + Rxy_threshold * ...
                                        threshold_vec(3,:);
     peak = zeros(1,9);         % Initialise a matrix to store results
   end

   %  Locate energy peaks
   disp('Finding peaks...');
   [p_out] = find_peak(lofar,f,t,threshold,time_duration);

   %%% Analysis of Peaks %%%

   %  Compute the df_dt for each of the peak and use this information
   %  to synthetically generated Power Spectra for different
   %  velocities.  Find best match using correlation.

   [m,n]= size(p_out);

   peak_count=peak_count + m;

   if m > 0
      disp([num2str(m),' peaks found.']);
      disp(' ');

      for k = 1 : m

        disp(['Analysing peak ',num2str(k),'.']);
        [p_out(k,6),p_out(k,7)]=calc_df_dt(lofar, f, t, p_out(k,:));
        [p_out(k,8),p_out(k,9),p_out(k,7)] = peak_compare ...
              (lofar, f, t, p_out(k,:),time_duration,threshold_vec);

          if p_out(k,7) == 2
          %  Plot Pressure-time graph

            detection_count = detection_count + 1;
            start_time_I = find (y(:,1) >= ...
                      (p_out(k,2) - 2*time_duration),1,'first');
            end_time_I   = find (y(:,1) >  ...
                       (p_out(k,2) + 2*time_duration),1,'first');

            subplot(2,2,1);
            plot (y (start_time_I :end_time_I ,1),...
                              y(start_time_I:end_time_I,2));
            xlabel('Time (s)');
            ylabel('Sound Pressure (AU)');
            grid on;
```

```
            title ('Sound Pressure vs Time Plot');

            clear start_time_I end_time_I;
           end
        end
    end

%  Copy result to Master Table
    if j==1
        peak = p_out;
    else
        peak = [peak ; p_out];
    end

end
fclose(fid);                    % close ASCII file


%  Generate output report

flag_interpret = char('No Doppler Shift.  df/dt inadmissible.',...
    'No Doppler Shift Detected.  Rxy less than Threshold.',...
    'Contact with Doppler Shift found.');

outfile=[infile(1:9),'_results.txt'];          % Name of output file

fid=fopen(outfile,'w');

fprintf(fid,'Results from analysis of %s.\n\n',infile);
fprintf(fid,'Threshold settings : %6.2f.\t Rxy_threshold : %6.2f.\n', ... threshold_setting
,Rxy_threshold);

fprintf(fid,'Threshold for energy based detection = ...
                                %7.4f.\n',threshold);
fprintf(fid,'No of peaks found = %4.0f.\n',peak_count);
fprintf(fid,'No of Doppler Shifts detected = ...
                                                %3.0f.\n\n',detection_count);
fprintf(fid,'Start time : %s.\n\n',start_time);
fprintf(fid,'Peak No.      Time        Freq       Result        ...
                            Velocity      Rxy        Range \n');

for i = 1 : peak_count

    fprintf(fid,'%3.0f\t    \t    %7.2f\t    %7.2f\t    %s\t    ',...                                    (i),
peak(i,2),peak(i,3),flag_interpret((peak(i,7)+1),:));

  if peak(i,7)== 2

      R_0 = -((peak(i,8)^2)/(peak(i,6)))*(peak(i,3)/343);

      fprintf(fid,'%7.2f\t %7.2f\t %7.2f  \n',peak(i,8),peak(i,9),R_0);
  else
```

```
    fprintf(fid,'\n');
  end

end

fclose(fid);

disp(['Analysis Completed.  Results written to file "',outfile,""]);

%%%%%%%%%%%%%%%%  End of Program %%%%%%%%%%%%%%%%%%%%%%%%%%%%
```

APPENDIX C. MATLAB FUNCTION CODE : time_to_freq.m

```
function [f,t,lofar] = time_to_freq(y,Fs,del_f,int_t)
%  Computes the Power Spectral Density.

%  Purpose : This function performs the Fourier Transform of the
%  time-domain input y and returns the Power Spectral Density estimate
%  via Welch's method.

%  Input Variables
%    y      :  signal in time domain.
%    Fs     :  Sampling Frequency.
%    del_f  :  Desired Frequency spacing (freq resolution)
%    int_t  :  Integration time


%  Output Variables
%    lofar      :  Matrix of Power Spectrum .
%    f          :  Frequency Matrix for 'lofar' (x-axis)
%    t          :  Time matrix for 'lofar' (y-axis)

%  Local Variables
%    NFFT       :  Number of FFTs to perform
%    avg        :  No of averages.
%    chunk      :  Length of each time domain data segment
%    N          :  No. of time domain data segments

%  Functions called  :  none

%  Written by Prof. Daphne Kapolka, NPS
%  Adapted by How Whye Keong, NPS, 10 Feb 2009

%%%%%%%%%%%%%%%%%%%%%%%%%%%%%%%%%%%%%%%%%%%%%%%%%%%%%%%%%%%

   NFFT = 2^(ceil(log2(Fs/del_f)));        %  No. of FFTs
   window = hamming(NFFT);

   time_FFT = NFFT/Fs;

   avg = floor(int_t/time_FFT);       %  No of averages

    if avg == 0
       avg = 1;
    end

   chunk = NFFT*avg;    %   length of time data needed to get averages

   N = floor(length(y)/chunk);     % Total number of chunks available

   lofar = ones(N,NFFT/2+1);       % initialize matrix for speed
```

```
x = ones(1,NFFT/2+1);
t = (1:N)' * (chunk/Fs);        %  time corresponding to end of the
                                                    %  ith chunk


for i = 1:N     % calculate avg power spectrum for each chunk

    low = 1+(i-1)*chunk;
    high = i*chunk;

    [x,f] = pwelch(y(low:high),window,NFFT/2, NFFT,Fs);

    x = x';

    lofar(i,:)=x;    % make the ith row of the lofargram the power
                                        % spectrum for that chunk

end

%%%%%%%%%%%%%%%% End of function %%%%%%%%%%%%%%%%
```

APPENDIX D. MATLAB FUNCTION CODE : find_peak.m

```
function [peak] = find_peak(lofar_func,f_func,t_func,threshold,time_duration)
%  Search for peaks in the frequency domain of input signal.

%  Purpose : This function search for energy peaks in a signal in the
%  input frequency - time matrix (lofar_func).  This is done by summing
%  the total energy across all frequenies within a time band and
%  compare it to a user determined threshold.  The function also search
%  for the tonal (frequecy) with the highest magnitude above a preset
%  frequency.

%  The function's output is a matrix (peak) containing the time (peak
%  time) when the threshold was exceeded and strongest tonal's
%  frequency.

%  Input Variables
%    lofar_func :  signal in frequency domain.
%    f_func     :  frequency matrix of signal corresponding to %
lofar_func.
%    t_func     :  time matrix of signal corresponding to lofar_func
%    threshold  :  The threshold for peak detection.
%    time_duration : The length of passage.  Used to determine how the
%                    length of buffer segment.

%  Output Variables
%    peak       :  Matrix with time(peak) when threshold was exceeded.
%    Structure of Matrix 'peak'

%      Peak No.     Time     Frequency    Time_index  Frequency_Index
%      --------     -----    ---------    ----------  ---------------

%  Local Variables
%    threshold             :  Threshold signal compared to
%    freq_min              :  Lower boundary to search for strongest tonal.
%    energy                :  Energy contained in a time band
%    num_peak              :  Count of instances where threshold is exceeded.
%    *.* _I                :  Index of parameter *.*.
%    a,n,i                 :  dummy variables and loop index.

%  Functions called  :  none

%  Comments :
%  Since the input time domain signal is padded at both ends with data
%  of length = time_duration, any peaks found in these regions is
%  omitted from the results since these regions overlaps with either
%  the previous or next data segment.

%  Written by How Whye Keong, NPS, 10 Feb 2009

%%%%%%%%%%%%%%%%%%%%%%%%%%%%%%%%%%%%%%%%%%%%%%%%%%%%%%%%%%%%%%%%%%%%%%%
```

```
freq_min = 90 ;    %  This is the lower boundary for the frequency band
                                %  to search in.


%%

energy = sum(lofar_func,2);     % sum total energy over all frequencies

%     figure;
%     plot(t_func,energy);
%     title('Total Energy vs Time');
%     xlabel('Time (s)');
%     ylabel('Total Energy');

%%
%  Find start & stop times where signal exceeds threshold and store in
%  matrix 'peak_times'

   over_threshold = energy > threshold;

   %  Locate start and stop times

   flag = over_threshold(1 : length(over_threshold)-1);
   flag_2 = over_threshold(2 : length(over_threshold));
   flag = xor(flag,flag_2);

   peak_times = t_func(flag);

   num_peak = floor(length(peak_times)/2);

%  Tabulate the peak time, strongest tonal Freq and their indexes.

n_time_seg = floor(time_duration/(t_func(2)-t_func(1)));
                                          %  time index of buffer section

peak = zeros (1, 5);   %  Output matrix

if num_peak > 0

   peak_counter = 1;
   for i = 1 : num_peak

      peak_st_I = find(t_func == peak_times ((2*i)-1));
      peak_et_I = find(t_func == peak_times (2*i));

      [a,n] = max (energy (peak_st_I : peak_et_I));
                                    % n = index of maxmimum energy in time span

      peak_time_I  = peak_st_I + n - 1;
                                                %  Index of peak time in t_func
```

```
      %  Search for strongest tonal in frequencies from freq_min Hz
           %  onwards.

      f_min_I = find (f_func > freq_min , 1 ,'first');
                                                                  %  Index of min_freq

      [a,n] = max (lofar_func(peak_time_I , f_min_I : ...
                                                                   length(f_func)));

      f_max_I = f_min_I + n - 1;

      %  Only record peaks outside of buffer region


      if (peak_time_I > n_time_seg) && (peak_time_I < ...
                                                          length(t_func)- n_time_seg)
                  %  Peak number
                    peak (peak_counter,1) = peak_counter;

                  %  Time of Peak
                    peak (peak_counter,2) = t_func(peak_time_I);

                  %  Freq of strongest tonal
            peak (peak_counter,3) = f_func(f_max_I);

                  %  Index
             peak (peak_counter,4) = peak_time_I;
             peak (peak_counter,5) = f_max_I;

          peak_counter          = peak_counter+1 ;
      end
   end
else
   peak = [];
   disp ('No Peaks found');
end

%%%%%%%%%%%%%%%%% end of function  %%%%%%%%%%%%%%%%
```

THIS PAGE INTENTIONALLY LEFT BLANK

APPENDIX E. MATLAB FUNCTION CODE : calc_df_dt.m

```
function [df_dt,flag] = calc_df_dt(lofar_func,f_func,t_func,peak_func)
%  Computes the rate of change of frequency.

%  Purpose : This function computes the rate of change of frequency of
%  a tonal.  "Tracking" of the tonal through time is based on the
%  assumption that within the time period of interest and in the
%  vicinity  of the tonal's frequency, the tonal will have the highest
%  magnitude.

%  Input Variables
%    lofar      :    Matrix of Power Spectrum
%    f_func     :    Frequency matrix of power spectrum
%    t_funct    :    time matrix of power spectrum
%    f_func and t_func is used to compute frequency resolution and time
%    spacing data points

%    peak_func  :    matrix containing information on time and
%                    frequency of tonal of interest.

%                    Format as follows :
%
%    Peak No.     Time     Frequency     Time_index    Frequency_Index
%    --------     -----    ---------     ----------    ---------------

%  Output Variables
%   df_dt     :  The mean rate of change of freq. for tonal of interest

%  Local Variables
%   max_v        :  Maximum expected velocity.  Affects the freq range
%                around tonal in which changes are looked for.
%   del_f, int_t  :  frequency and time between data points.
%   span         :  No. of bins based on max_v and del_f.
%   no_point     :  No. of time periods before/after t0
%                used to calculate mean df/dt.

%  Functions called  :  none

%  Written by How Whye Keong, NPS, 11 Feb 2009

%%%%%%%%%%%%%%%%%%%%%%%%%%%%%%%%%%%%%%%%%%%%%%%%%%%%%%%%%%%%%%%%%%%%%%%%%%%%

max_v    = 100;            %  Max velocity of contacts expected (m/s)
c_air    = 343;            %  Speed of sound
no_point = 1;              %  Number of points to base df/dt calculations

%  Calculate freq and time spacing.

  int_t = t_func(2)- t_func(1);
```

```
   del_f = f_func(2)- f_func(1) ;

%  Calculate the many "bins" to track tonal of interest.

   span = (max_v/c_air) * peak_func(1,3) ;
   span = ceil (span/del_f);

%  Locate peaks.  Search for the strongest tonal in the vicinity of
%  tonal's frequency and time.  'time intervals' before and after
%  tonal's time is as input in 'no_point'.

a = zeros (1, (length(no_point)*2 + 1));
                    % matrix to store freq index of tonal.

a(no_point + 1) = peak_func (1,5);  %  tonal's freq_index.

%  locate tonals before and after t0

for i = 1 : no_point

    [b,n] = max (lofar_func( (peak_func(1,4)-i) ,  ...
                                        peak_func(1,5) : peak_func(1,5)+ span));
    a(no_point + 1 - i) = peak_func(1,5) + n-1;

    [c,m] = max (lofar_func( (peak_func(1,4)+i) , ...
                                    peak_func(1,5)- span : peak_func(1,5)));
    a(no_point + 1 + i) = peak_func(1,5) - span + m-1;

end

df_dt = diff(a) * del_f / int_t ;

%  Check that df_dt is negative for all points.
    b = (df_dt >= 0);    %  Flag if positive
    b = sum(b);

    if b == 0
        flag = 1;       %  All negative
    else
        flag = 0;       %  Not all negative
    end

df_dt = mean (df_dt);

%%%%%%%%%%%%%%%%%%%% end of function  %%%%%%%%%%%%%%%%%%
```

APPENDIX F. MATLAB FUNCTION CODE : peak_compare.m

```
function [v_out,R_out,plot_check] =
peak_compare(lofar,f_func,t_func,peak_func,time_duration,threshold_vec)
%  Finds velocity through use of correlation on input Power Spectrum.

%  Purpose : This function finds the velocity of best match to an input
%  power spectral through the use of correlation against templates of
%  synthetic generated Doppler Shift patterns.  These templates are of
%  generated based on inputs df/dt and velocity.  The Correlation Rxy
%  is  tabulated for an array of velocities.  Graph of Rxy vs velocity
%  is plotted and the velocity corresponding to the highest Rxy is
%  output from the function.

%  Input Variables
%   lofar                :  Power Spectral Density Matrix
%   f_func, t_func       :  Freq and time array corresponding to lofar
%   peak_func            :  matrix containing information on time, frequency
%                           and df/dt of tonal of interest.  Format as follows :
%
%     Peak No. Time  Frequency  Time_index  Frequency_Index  df/dt
%     -------- ----  ---------  ----------  ---------------  ------

%  Output Variables
%   v_out                :       Velocity of best match
%   R_out                :       Rxy value of best match for v_out

%  Local Variables
%   time_duration        :  Total length of time of signal to analyse (s)
%   n,m,span             :  counting indexes.
%   total                :  Index of correlation values
%   Rxy                  :  Correlation values


%  Functions called  :  generate_template


%  Written by How Whye Keong, NPS, 11 Feb 2009%%%%%%%%%%%%%%

%  Definition of constants

tic

max_v        = 100;       %  Max velocity of contacts expected (m/s)
c_air        = 343;       %  Speed of sound


%%%  Extract the segment of 'interest' around tonal of interest %%%

%  Translate time duration into no. of time blocks before CPA
```

```
n = floor((time_duration /(t_func(2) - t_func(1))));

%  To ensure that the duration of the template signal to be generated
%  is exactly of the same length as that of the original signal.

time_duration = (n*2*(t_func(2) - t_func(1)));


%  Calculate number of frequency blocks.
%  An arbitary factor of 1.3 is used to extend span to ensure that the
%  entire section of the Doppler shift pattern is captured

span = ((max_v/c_air) * peak_func(1,3)) / (f_func(2)-f_func(1));
span = ceil(1.3*span);

%  Extract section of interest from main lofar matrix

f0_I = peak_func (1,5);     %  Index of freq of interest
t0_I = peak_func (1,4);     %  Index of time of interest

t_sect = t_func(t0_I - n : t0_I + n);
f_sect = f_func(f0_I - (span) : f0_I + (span));
lofar_sect = lofar(t0_I - n : t0_I + n , f0_I - span : f0_I + span);

[m n] = size (lofar_sect);

%  Normalise lofar_sect.

norm_fac = sum(lofar_sect,2);
N = norm_fac * ones(1,n);
lofar_sect = lofar_sect ./ N ;


%%%  Correlate lofar_sect to possible templates  %%%

vel_min = 30;
vel_max = 100;

%  Compute velocity resolution based on freq resolution

vel_resolution = (1/peak_func(1,3))* c_air;
N = floor((vel_max-vel_min)/vel_resolution);

vel = linspace (vel_min , vel_max, N);

%  Generate the template based on df/dt and carry out correlation.

df_dt = peak_func (1,6);
```

```
if (df_dt >= 0) || (peak_func (1,7)==0) ;

    disp('No Doppler Shift.  df/dt inadmissible');
    v_out = 99.999;
    R_out = 0;
    plot_check = 0;

else

    total = zeros (1, length(vel));

    for j = 1 : length(vel)

        v = vel(j);

        [lofar_template] = generate_template(v, time_duration , ...
                                                        25000 ,peak_func(3),df_dt);
        lofar_template = lofar_template( : , f0_I - span : f0_I ...
                                                                    + span);

        Rxy = xcorr2(lofar_sect, lofar_template);
        total(j)= max(max(Rxy));

    end

    index = ((max(total)) == total);
    Rxy   = total(index);

    %  determine frequency band of f_0 and set threshold.
    diff_vec =  threshold_vec (1,:) - peak_func(1,3);
    [m n] = min(abs(diff_vec));


    if Rxy >= threshold_vec(4,n)

        v_out = vel(index);
        R_out = total(index);

        disp(' ');
        disp(['Contact with Doppler Shift found at t = ',...
            num2str(peak_func(1,2)),'s.']);
        disp(['Velocity of contact is ',num2str(v_out),' m/s.']);

        %  Produce plot
            plot_check = 2;
            lofar_db_1 = 10* log10(lofar);
            lofar_db = 10*log10 (lofar_sect);
```

```
        figure;

        subplot(2,2,2)
        pcolor (f_func(1:400),...
           t_func(peak_func(1,4) - 10 : ...
             peak_func(1,4) + 10),...
               lofar_db_1(peak_func(1,4) - 10 :...
                 peak_func(1,4) + 10, 1:400));
        shading interp
        xlabel('Frequency (Hz)')
        ylabel('Time (s)')
        colorbar
        title('LOFARgram');

        subplot(2,2,3)
        pcolor (f_sect,t_sect,lofar_db)
        shading interp
        xlabel('Frequency (Hz)')
        ylabel('Time (s)')
        colorbar
        grid on;
        title('Tonal Analysed');

        subplot(2,2,4)
        plot(vel,total);
        xlabel('Velocity (m/s)');
        ylabel('Rxy');
        grid on;
        title('Plot of Rxy vs Velocity');
        annotation('textbox','String',{'Threshold :',...
                                              num2str(threshold_vec(4,n),4)},...
                                                    'FitHeightToText','off',...
                                'Position',[0.8422 0.3773 0.05937 0.05674]);


    else

        v_out = vel(index);
        R_out = total(index);
        plot_check = 1;

        disp(' ')
        disp('No Doppler Shift Detected.  Rxy less than Threshold');

    end
end

toc

 %%%%%%%%%%%%%%%% End of Function  %%%%%%%%%%%%%%%%
```

APPENDIX G. MATLAB FUNCTION CODE : generate_template.m

```
function [lofar_out] = generate_template(vel,t_duration,Fs,f_0,df_dt)
%  This function generates template with Doppler Shift pattern based of
%  input velocity.

%  Purpose : This function generates a template of Doppler shift
%          pattern.
%          The pattern is centred on the input freq f_0 and df/dt.

%         The function uses these two parameters to generate the
%          time-domain signal.  The power spectrum is computed using
%          the 'time_to_freq' function.

%  Input Variables
%    vel               :  Velocity
%    t_duration          :  length of sample to generate in time
%    f_0               :  Frequency a CPA
%    df/dt             :  Rate of change at CPA

%  Output Variables
%    lofar_out :       Power Spectrum with Doppler Shift pattern
%    f,t       :       frequency and time matrix correponding to
%                      lofar_out

%  Local Variables
%    t         :       Time (s)
%    f         :       Frequency (Hz)
%    r         :       Range (m)
%    p         :       Pressure (pa)

%  Functions called  :  time_to_freq

%  Written by How Whye Keong, NPS, 11 Feb 2009  %%%%%%%%%%%%%%%%%%%%%%%%

    c     = 343;          %  Sound of Speed in Air
    A     = 10;           %  Amplitude (Arbitary)

    t = linspace ((-t_duration/2),(t_duration/2),(t_duration * Fs)) ;

%   Calculate the Pressure as function of time.

%    r = vel * sqrt( (t.^2)+((vel*f_0)/(c * df_dt))^2);
%                          as required to check CPA range


  f = f_0 * (1 - ((vel.*t)./ (sqrt( (c*t).^2 + (vel*f_0/df_dt)^2))));

  p  = A * sin(2*pi.*f.*t);
```

```
%  Convert the pressure-time profile into frequency domain

   [f,t,lofar_out] = time_to_freq(p',Fs,4,1);

%%%%%%%%%%%%%%%%% End of Function %%%%%%%%%%%%%%%%%%
```

APPENDIX H. OUTPUT RESULT REPORTS FROM auto_Doppler_detector.m

1. Run 1 – Threshold $\mu + 15\sigma$, R_{xy} Threshold $\mu_r + 0.5\sigma_r$

Results from analysis of 07_aug_08.txt.

Threshold for energy based detection = 0.1093.
No of peaks found = 131.
No of Doppler Shifts detected = 10.

Start time : 8/7/2008 10:20:52.55.

Peak No.	Time	Freq	Result	Velocity	Rxy	Range		
1	74.71	122.07	Contact with Doppler Shift found.	48.26	56.43	106.80		
2	623.42	94.60	Contact with Doppler Shift found.	53.33	51.63	168.48		
3	814.13	125.12	No Doppler Shift. df/dt inadmissible.					
4	816.10	91.55	No Doppler Shift Detected. Rxy less than Threshold.					
5	818.07	122.07	No Doppler Shift. df/dt inadmissible.					
6	822.98	103.76	No Doppler Shift Detected. Rxy less than Threshold.					
7	835.76	115.97	No Doppler Shift Detected. Rxy less than Threshold.					
8	879.01	103.76	No Doppler Shift Detected. Rxy less than Threshold.					
9	1089.56	103.76	No Doppler Shift Detected. Rxy less than Threshold.					
10	1092.51	109.86	No Doppler Shift. df/dt inadmissible.					
11	1215.56	112.92	No Doppler Shift. df/dt inadmissible.					
12	1230.30	103.76	No Doppler Shift. df/dt inadmissible.					
13	1232.27	103.76	No Doppler Shift. df/dt inadmissible.					
14	1276.51	115.97	No Doppler Shift. df/dt inadmissible.					
15	1422.98	112.92	No Doppler Shift Detected. Rxy less than Threshold.					
16	1457.39	91.55	No Doppler Shift Detected. Rxy less than Threshold.					
17	1490.81	109.86	No Doppler Shift. df/dt inadmissible.					
18	1516.54	125.12	Contact with Doppler Shift found.	41.67	19.14	17.00		
19	1519.49	103.76	No Doppler Shift Detected. Rxy less than Threshold.					
20	1526.37	115.97	No Doppler Shift Detected. Rxy less than Threshold.					
21	1575.52	122.07	No Doppler Shift. df/dt inadmissible.					
22	1582.37	137.33	Contact with Doppler Shift found.	61.11	47.38	321.10		
23	1610.91	115.97	No Doppler Shift. df/dt inadmissible.					
24	1619.76	100.71	No Doppler Shift Detected. Rxy less than Threshold.					
25	1636.47	91.55	No Doppler Shift. df/dt inadmissible.					
26	1659.08	91.55	No Doppler Shift Detected. Rxy less than Threshold.					
27	1795.73	250.24	Contact with Doppler Shift found.	32.80	8.36	12.97		
28	1805.73	97.66	No Doppler Shift Detected. Rxy less than Threshold.					
29	1811.63	91.55	No Doppler Shift Detected. Rxy less than Threshold.					

30	1859.80	125.12	No Doppler Shift. df/dt inadmissible.			
31	1872.58	125.12	No Doppler Shift. df/dt inadmissible.			
32	1874.54	97.66	No Doppler Shift. df/dt inadmissible.			
33	1924.68	137.33	Contact with Doppler Shift found.	48.15	30.36	85.42
34	1931.56	109.86	No Doppler Shift. df/dt inadmissible.			
35	1943.35	97.66	No Doppler Shift Detected. Rxy less than Threshold.			
36	1946.30	134.28	Contact with Doppler Shift found.	38.08	18.78	16.62
37	1950.24	97.66	No Doppler Shift Detected. Rxy less than Threshold.			
38	1957.12	94.60	No Doppler Shift. df/dt inadmissible.			
39	2004.30	125.12	No Doppler Shift. df/dt inadmissible.			
40	2028.88	109.86	No Doppler Shift Detected. Rxy less than Threshold.			
41	2214.85	91.55	No Doppler Shift Detected. Rxy less than Threshold.			
42	2119.46	131.23	Contact with Doppler Shift found.	44.00	46.24	119.29
43	2223.69	125.12	No Doppler Shift. df/dt inadmissible.			
44	2229.59	91.55	No Doppler Shift Detected. Rxy less than Threshold.			
45	2232.54	125.12	No Doppler Shift. df/dt inadmissible.			
46	2263.02	91.55	No Doppler Shift. df/dt inadmissible.			
47	2269.90	94.60	No Doppler Shift Detected. Rxy less than Threshold.			
48	2305.29	119.02	No Doppler Shift Detected. Rxy less than Threshold.			
49	2311.18	100.71	No Doppler Shift Detected. Rxy less than Threshold.			
50	2371.15	91.55	No Doppler Shift Detected. Rxy less than Threshold.			
51	2390.81	97.66	No Doppler Shift Detected. Rxy less than Threshold.			
52	2467.66	100.71	No Doppler Shift Detected. Rxy less than Threshold.			
53	2601.35	97.66	No Doppler Shift. df/dt inadmissible.			
54	2611.18	91.55	No Doppler Shift Detected. Rxy less than Threshold.			
55	2616.10	91.55	No Doppler Shift. df/dt inadmissible.			
56	2632.81	109.86	No Doppler Shift Detected. Rxy less than Threshold.			
57	2635.76	97.66	No Doppler Shift Detected. Rxy less than Threshold.			
58	2642.64	106.81	No Doppler Shift Detected. Rxy less than Threshold.			
59	2656.40	97.66	No Doppler Shift. df/dt inadmissible.			
60	2692.78	161.74	No Doppler Shift. df/dt inadmissible.			
61	2716.54	106.81	No Doppler Shift. df/dt inadmissible.			
62	2726.37	109.86	No Doppler Shift Detected. Rxy less than Threshold.			
63	2735.22	125.12	No Doppler Shift. df/dt inadmissible.			
64	2739.15	125.12	No Doppler Shift. df/dt inadmissible.			
65	2754.88	161.74	No Doppler Shift. df/dt inadmissible.			
66	2790.27	112.92	No Doppler Shift Detected. Rxy less than Threshold.			
67	2796.17	91.55	No Doppler Shift. df/dt inadmissible.			
68	2822.71	91.55	No Doppler Shift Detected. Rxy less than Threshold.			
69	2827.63	125.12	No Doppler Shift. df/dt inadmissible.			
70	2849.25	112.92	No Doppler Shift Detected. Rxy less than Threshold.			
71	2865.96	125.12	No Doppler Shift. df/dt inadmissible.			
72	2873.83	91.55	No Doppler Shift. df/dt inadmissible.			
73	2882.68	91.55	No Doppler Shift Detected. Rxy less than Threshold.			
74	2920.03	97.66	No Doppler Shift. df/dt inadmissible.			
75	2938.71	106.81	No Doppler Shift Detected. Rxy less than Threshold.			

76	2943.62	97.66	No Doppler Shift Detected. Rxy less than Threshold.			
77	2948.54	91.55	No Doppler Shift Detected. Rxy less than Threshold.			
78	2956.40	125.12	No Doppler Shift. df/dt inadmissible.			
79	2971.15	91.55	No Doppler Shift. df/dt inadmissible.			
80	2983.93	125.12	No Doppler Shift. df/dt inadmissible.			
81	2987.86	91.55	No Doppler Shift Detected. Rxy less than Threshold.			
82	3008.68	97.66	No Doppler Shift Detected. Rxy less than Threshold.			
83	3011.63	125.12	No Doppler Shift. df/dt inadmissible.			
84	3013.59	100.71	No Doppler Shift Detected. Rxy less than Threshold.			
85	3023.42	91.55	No Doppler Shift Detected. Rxy less than Threshold.			
86	3037.19	97.66	No Doppler Shift. df/dt inadmissible.			
87	3048.00	112.92	No Doppler Shift Detected. Rxy less than Threshold.			
88	3050.95	128.17	No Doppler Shift Detected. Rxy less than Threshold.			
89	3056.85	122.07	No Doppler Shift Detected. Rxy less than Threshold.			
90	3060.78	94.60	No Doppler Shift Detected. Rxy less than Threshold.			
91	3069.63	91.55	No Doppler Shift. df/dt inadmissible.			
92	3073.56	103.76	No Doppler Shift Detected. Rxy less than Threshold.			
93	3075.52	91.55	No Doppler Shift Detected. Rxy less than Threshold.			
94	3078.47	115.97	No Doppler Shift Detected. Rxy less than Threshold.			
95	3083.39	100.71	No Doppler Shift Detected. Rxy less than Threshold.			
96	3095.19	122.07	No Doppler Shift Detected. Rxy less than Threshold.			
97	3105.02	91.55	No Doppler Shift Detected. Rxy less than Threshold.			
98	3113.86	125.12	Contact with Doppler Shift found.	50.42	18.28	35.14
99	3121.73	97.66	No Doppler Shift Detected. Rxy less than Threshold.			
100	3125.66	125.12	No Doppler Shift. df/dt inadmissible.			
101	3204.30	112.92	No Doppler Shift Detected. Rxy less than Threshold.			
102	3209.22	97.66	No Doppler Shift Detected. Rxy less than Threshold.			
103	3259.35	125.12	No Doppler Shift. df/dt inadmissible.			
104	3264.27	91.55	No Doppler Shift. df/dt inadmissible.			
105	3278.03	106.81	No Doppler Shift Detected. Rxy less than Threshold.			
106	3280.98	106.81	No Doppler Shift Detected. Rxy less than Threshold.			
107	3286.88	97.66	No Doppler Shift Detected. Rxy less than Threshold.			
108	3292.78	115.97	No Doppler Shift Detected. Rxy less than Threshold.			
109	3296.71	125.12	No Doppler Shift. df/dt inadmissible.			
110	3300.81	125.12	No Doppler Shift. df/dt inadmissible.			
111	3303.76	91.55	No Doppler Shift Detected. Rxy less than Threshold.			
112	3314.58	97.66	No Doppler Shift Detected. Rxy less than Threshold.			
113	3317.53	106.81	No Doppler Shift. df/dt inadmissible.			
114	3348.98	100.71	No Doppler Shift Detected. Rxy less than Threshold.			
115	3381.42	97.66	No Doppler Shift Detected. Rxy less than Threshold.			
116	3385.35	97.66	No Doppler Shift. df/dt inadmissible.			
117	3389.29	100.71	No Doppler Shift. df/dt inadmissible.			
118	3424.68	283.81	Contact with Doppler Shift found.	30.00	9.79	19.19
119	3443.35	97.66	No Doppler Shift Detected. Rxy less than Threshold.			
120	3447.29	125.12	No Doppler Shift. df/dt inadmissible.			
121	3451.22	161.74	No Doppler Shift. df/dt inadmissible.			

122	3456.13	100.71	No Doppler Shift. df/dt inadmissible.
123	3461.05	97.66	No Doppler Shift Detected. Rxy less than Threshold.
124	3463.02	125.12	No Doppler Shift. df/dt inadmissible.
125	3485.62	125.12	No Doppler Shift. df/dt inadmissible.
126	3489.56	112.92	No Doppler Shift Detected. Rxy less than Threshold.
127	3511.18	109.86	No Doppler Shift Detected. Rxy less than Threshold.
128	3516.10	109.86	No Doppler Shift Detected. Rxy less than Threshold.
129	3522.98	125.12	No Doppler Shift. df/dt inadmissible.
130	3526.91	115.97	No Doppler Shift Detected. Rxy less than Threshold.
131	3622.44	125.12	No Doppler Shift. df/dt inadmissible.

2. Run 2 – Threshold μ + 15σ, Rxy Threshold $\mu_r + 1.0\sigma_r$

Results from analysis of 07_aug_08.txt.

Threshold for energy based detection = 0.1093.
No of peaks found = 131.
No of Doppler Shifts detected = 5.

Start time : 8/7/2008 10:20:52.55.

Peak No.	Time	Freq	Result	Velocity	Rxy	Range		
1	74.71	122.07	Contact with Doppler Shift found.			48.26	56.43	106.80
2	623.42	94.60	Contact with Doppler Shift found.			53.33	51.63	168.48
3	814.13	125.12	No Doppler Shift. df/dt inadmissible.					
4	816.10	91.55	No Doppler Shift Detected. Rxy less than Threshold.					
5	818.07	122.07	No Doppler Shift. df/dt inadmissible.					
6	822.98	103.76	No Doppler Shift Detected. Rxy less than Threshold.					
7	835.76	115.97	No Doppler Shift Detected. Rxy less than Threshold.					
8	879.01	103.76	No Doppler Shift Detected. Rxy less than Threshold.					
9	1089.56	103.76	No Doppler Shift Detected. Rxy less than Threshold.					
10	1092.51	109.86	No Doppler Shift. df/dt inadmissible.					
11	1215.56	112.92	No Doppler Shift. df/dt inadmissible.					
12	1230.30	103.76	No Doppler Shift. df/dt inadmissible.					
13	1232.27	103.76	No Doppler Shift. df/dt inadmissible.					
14	1276.51	115.97	No Doppler Shift. df/dt inadmissible.					
15	1422.98	112.92	No Doppler Shift Detected. Rxy less than Threshold.					
16	1457.39	91.55	No Doppler Shift Detected. Rxy less than Threshold.					
17	1490.81	109.86	No Doppler Shift. df/dt inadmissible.					
18	1516.54	125.12	No Doppler Shift Detected. Rxy less than Threshold.					
19	1519.49	103.76	No Doppler Shift Detected. Rxy less than Threshold.					
20	1526.37	115.97	No Doppler Shift Detected. Rxy less than Threshold.					
21	1575.52	122.07	No Doppler Shift. df/dt inadmissible.					
22	1582.37	137.33	Contact with Doppler Shift found.			61.11	47.38	321.10
23	1610.91	115.97	No Doppler Shift. df/dt inadmissible.					
24	1619.76	100.71	No Doppler Shift Detected. Rxy less than Threshold.					
25	1636.47	91.55	No Doppler Shift. df/dt inadmissible.					
26	1659.08	91.55	No Doppler Shift Detected. Rxy less than Threshold.					
27	1795.73	250.24	No Doppler Shift Detected. Rxy less than Threshold.					
28	1805.73	97.66	No Doppler Shift Detected. Rxy less than Threshold.					
29	1811.63	91.55	No Doppler Shift Detected. Rxy less than Threshold.					
30	1859.80	125.12	No Doppler Shift. df/dt inadmissible.					
31	1872.58	125.12	No Doppler Shift. df/dt inadmissible.					
32	1874.54	97.66	No Doppler Shift. df/dt inadmissible.					
33	1924.68	137.33	Contact with Doppler Shift found.			48.15	30.36	85.42
34	1931.56	109.86	No Doppler Shift. df/dt inadmissible.					

35	1943.35	97.66	No Doppler Shift Detected. Rxy less than Threshold.			
36	1946.30	134.28	No Doppler Shift Detected. Rxy less than Threshold.			
37	1950.24	97.66	No Doppler Shift Detected. Rxy less than Threshold.			
38	1957.12	94.60	No Doppler Shift. df/dt inadmissible.			
39	2004.30	125.12	No Doppler Shift. df/dt inadmissible.			
40	2028.88	109.86	No Doppler Shift Detected. Rxy less than Threshold.			
41	2214.85	91.55	No Doppler Shift Detected. Rxy less than Threshold.			
42	2119.46	131.23	Contact with Doppler Shift found.	44.00	46.24	119.29
43	2223.69	125.12	No Doppler Shift. df/dt inadmissible.			
44	2229.59	91.55	No Doppler Shift Detected. Rxy less than Threshold.			
45	2232.54	125.12	No Doppler Shift. df/dt inadmissible.			
46	2263.02	91.55	No Doppler Shift. df/dt inadmissible.			
47	2269.90	94.60	No Doppler Shift Detected. Rxy less than Threshold.			
48	2305.29	119.02	No Doppler Shift Detected. Rxy less than Threshold.			
49	2311.18	100.71	No Doppler Shift Detected. Rxy less than Threshold.			
50	2371.15	91.55	No Doppler Shift Detected. Rxy less than Threshold.			
51	2390.81	97.66	No Doppler Shift Detected. Rxy less than Threshold.			
52	2467.66	100.71	No Doppler Shift Detected. Rxy less than Threshold.			
53	2601.35	97.66	No Doppler Shift. df/dt inadmissible.			
54	2611.18	91.55	No Doppler Shift Detected. Rxy less than Threshold.			
55	2616.10	91.55	No Doppler Shift. df/dt inadmissible.			
56	2632.81	109.86	No Doppler Shift Detected. Rxy less than Threshold.			
57	2635.76	97.66	No Doppler Shift Detected. Rxy less than Threshold.			
58	2642.64	106.81	No Doppler Shift Detected. Rxy less than Threshold.			
59	2656.40	97.66	No Doppler Shift. df/dt inadmissible.			
60	2692.78	161.74	No Doppler Shift. df/dt inadmissible.			
61	2716.54	106.81	No Doppler Shift. df/dt inadmissible.			
62	2726.37	109.86	No Doppler Shift Detected. Rxy less than Threshold.			
63	2735.22	125.12	No Doppler Shift. df/dt inadmissible.			
64	2739.15	125.12	No Doppler Shift. df/dt inadmissible.			
65	2754.88	161.74	No Doppler Shift. df/dt inadmissible.			
66	2790.27	112.92	No Doppler Shift Detected. Rxy less than Threshold.			
67	2796.17	91.55	No Doppler Shift. df/dt inadmissible.			
68	2822.71	91.55	No Doppler Shift Detected. Rxy less than Threshold.			
69	2827.63	125.12	No Doppler Shift. df/dt inadmissible.			
70	2849.25	112.92	No Doppler Shift Detected. Rxy less than Threshold.			
71	2865.96	125.12	No Doppler Shift. df/dt inadmissible.			
72	2873.83	91.55	No Doppler Shift. df/dt inadmissible.			
73	2882.68	91.55	No Doppler Shift Detected. Rxy less than Threshold.			
74	2920.03	97.66	No Doppler Shift. df/dt inadmissible.			
75	2938.71	106.81	No Doppler Shift Detected. Rxy less than Threshold.			
76	2943.62	97.66	No Doppler Shift Detected. Rxy less than Threshold.			
77	2948.54	91.55	No Doppler Shift Detected. Rxy less than Threshold.			
78	2956.40	125.12	No Doppler Shift. df/dt inadmissible.			
79	2971.15	91.55	No Doppler Shift. df/dt inadmissible.			
80	2983.93	125.12	No Doppler Shift. df/dt inadmissible.			

81	2987.86	91.55	No Doppler Shift Detected. Rxy less than Threshold.
82	3008.68	97.66	No Doppler Shift Detected. Rxy less than Threshold.
83	3011.63	125.12	No Doppler Shift. df/dt inadmissible.
84	3013.59	100.71	No Doppler Shift Detected. Rxy less than Threshold.
85	3023.42	91.55	No Doppler Shift Detected. Rxy less than Threshold.
86	3037.19	97.66	No Doppler Shift. df/dt inadmissible.
87	3048.00	112.92	No Doppler Shift Detected. Rxy less than Threshold.
88	3050.95	128.17	No Doppler Shift Detected. Rxy less than Threshold.
89	3056.85	122.07	No Doppler Shift Detected. Rxy less than Threshold.
90	3060.78	94.60	No Doppler Shift Detected. Rxy less than Threshold.
91	3069.63	91.55	No Doppler Shift. df/dt inadmissible.
92	3073.56	103.76	No Doppler Shift Detected. Rxy less than Threshold.
93	3075.52	91.55	No Doppler Shift Detected. Rxy less than Threshold.
94	3078.47	115.97	No Doppler Shift Detected. Rxy less than Threshold.
95	3083.39	100.71	No Doppler Shift Detected. Rxy less than Threshold.
96	3095.19	122.07	No Doppler Shift Detected. Rxy less than Threshold.
97	3105.02	91.55	No Doppler Shift Detected. Rxy less than Threshold.
98	3113.86	125.12	No Doppler Shift Detected. Rxy less than Threshold.
99	3116.81	125.12	No Doppler Shift Detected. Rxy less than Threshold.
100	3121.73	97.66	No Doppler Shift Detected. Rxy less than Threshold.
101	3125.66	125.12	No Doppler Shift. df/dt inadmissible.
102	3204.30	112.92	No Doppler Shift Detected. Rxy less than Threshold.
103	3209.22	97.66	No Doppler Shift. df/dt inadmissible.
105	3264.27	91.55	No Doppler Shift. df/dt inadmissible.
106	3278.03	106.81	No Doppler Shift Detected. Rxy less than Threshold.
107	3280.98	106.81	No Doppler Shift Detected. Rxy less than Threshold.
108	3286.88	97.66	No Doppler Shift Detected. Rxy less than Threshold.
109	3292.78	115.97	No Doppler Shift Detected. Rxy less than Threshold.
110	3296.71	125.12	No Doppler Shift. df/dt inadmissible.
111	3300.81	125.12	No Doppler Shift. df/dt inadmissible.
112	3303.76	91.55	No Doppler Shift Detected. Rxy less than Threshold.
113	3314.58	97.66	No Doppler Shift Detected. Rxy less than Threshold.
114	3317.53	106.81	No Doppler Shift. df/dt inadmissible.
115	3348.98	100.71	No Doppler Shift Detected. Rxy less than Threshold.
116	3381.42	97.66	No Doppler Shift Detected. Rxy less than Threshold.
117	3385.35	97.66	No Doppler Shift. df/dt inadmissible.
118	3389.29	100.71	No Doppler Shift. df/dt inadmissible.
119	3443.35	97.66	No Doppler Shift Detected. Rxy less than Threshold.
120	3447.29	125.12	No Doppler Shift. df/dt inadmissible.
121	3451.22	161.74	No Doppler Shift. df/dt inadmissible.
122	3456.13	100.71	No Doppler Shift. df/dt inadmissible.
123	3461.05	97.66	No Doppler Shift Detected. Rxy less than Threshold.
124	3463.02	125.12	No Doppler Shift. df/dt inadmissible.
125	3485.62	125.12	No Doppler Shift. df/dt inadmissible.

126	3489.56	112.92	No Doppler Shift Detected. Rxy less than Threshold.
127	3511.18	109.86	No Doppler Shift Detected. Rxy less than Threshold.
128	3516.10	109.86	No Doppler Shift Detected. Rxy less than Threshold.
129	3522.98	125.12	No Doppler Shift. df/dt inadmissible.
130	3526.91	115.97	No Doppler Shift Detected. Rxy less than Threshold.
131	3622.44	125.12	No Doppler Shift. df/dt inadmissible.

3. Run 3 – Threshold μ + 20σ, Rxy Threshold $\mu_r + 0.5\sigma_r$

Results from analysis of 07_aug_08.txt.

Threshold for energy based detection = 0.1380.
No of peaks found = 113.
No of Doppler Shifts detected = 7.

Start time : 8/7/2008 10:20:52.55.

Peak No.	Time	Freq	Result	Velocity	Rxy	Range	
1	74.71	122.07	Contact with Doppler Shift found.		48.26	56.43	106.80
2	623.42	94.60	Contact with Doppler Shift found.		53.33	51.63	168.48
3	814.13	125.12	No Doppler Shift. df/dt inadmissible.				
4	816.10	91.55	No Doppler Shift Detected. Rxy less than Threshold.				
5	818.07	122.07	No Doppler Shift. df/dt inadmissible.				
6	822.98	103.76	No Doppler Shift Detected. Rxy less than Threshold.				
7	835.76	115.97	No Doppler Shift Detected. Rxy less than Threshold.				
8	1089.56	103.76	No Doppler Shift Detected. Rxy less than Threshold.				
9	1092.51	109.86	No Doppler Shift. df/dt inadmissible.				
10	1215.56	112.92	No Doppler Shift. df/dt inadmissible.				
11	1273.56	100.71	No Doppler Shift Detected. Rxy less than Threshold.				
12	1276.51	115.97	No Doppler Shift. df/dt inadmissible.				
13	1422.98	112.92	No Doppler Shift Detected. Rxy less than Threshold.				
14	1430.84	106.81	No Doppler Shift. df/dt inadmissible.				
15	1457.39	91.55	No Doppler Shift Detected. Rxy less than Threshold.				
16	1519.49	103.76	No Doppler Shift Detected. Rxy less than Threshold.				
17	1521.46	106.81	No Doppler Shift Detected. Rxy less than Threshold.				
18	1524.41	91.55	No Doppler Shift Detected. Rxy less than Threshold.				
19	1575.52	122.07	No Doppler Shift. df/dt inadmissible.				
20	1582.41	137.33	Contact with Doppler Shift found.		61.11	47.38	321.10
21	1619.76	100.71	No Doppler Shift Detected. Rxy less than Threshold.				
22	1653.18	94.60	No Doppler Shift Detected. Rxy less than Threshold.				
23	1794.74	225.83	No Doppler Shift Detected. Rxy less than Threshold.				
24	1805.73	97.66	No Doppler Shift Detected. Rxy less than Threshold.				
25	1811.63	91.55	No Doppler Shift Detected. Rxy less than Threshold.				
26	1872.58	125.12	No Doppler Shift. df/dt inadmissible.				
27	1874.54	97.66	No Doppler Shift. df/dt inadmissible.				
28	1924.68	137.33	Contact with Doppler Shift found.		48.15	30.36	85.42
29	1931.56	109.86	No Doppler Shift. df/dt inadmissible.				
30	1943.35	97.66	No Doppler Shift Detected. Rxy less than Threshold.				
31	1946.30	134.28	Contact with Doppler Shift found.		38.08	18.78	16.62
32	1957.12	94.60	No Doppler Shift. df/dt inadmissible.				
33	2004.30	125.12	No Doppler Shift. df/dt inadmissible.				
34	2028.88	109.86	No Doppler Shift Detected. Rxy less than Threshold.				
35	2119.49	131.23	Contact with Doppler Shift found.		44.00	46.24	119.29

36	2214.85	91.55	No Doppler Shift Detected. Rxy less than Threshold.
37	2216.81	97.66	No Doppler Shift Detected. Rxy less than Threshold.
38	2229.59	91.55	No Doppler Shift Detected. Rxy less than Threshold.
39	2232.54	125.12	No Doppler Shift. df/dt inadmissible.
40	2263.02	91.55	No Doppler Shift. df/dt inadmissible.
41	2269.90	94.60	No Doppler Shift Detected. Rxy less than Threshold.
42	2301.35	161.74	No Doppler Shift. df/dt inadmissible.
43	2305.29	119.02	No Doppler Shift Detected. Rxy less than Threshold.
44	2311.18	100.71	No Doppler Shift Detected. Rxy less than Threshold.
45	2371.15	91.55	No Doppler Shift Detected. Rxy less than Threshold.
46	2467.66	100.71	No Doppler Shift Detected. Rxy less than Threshold.
47	2601.35	97.66	No Doppler Shift. df/dt inadmissible.
48	2611.18	91.55	No Doppler Shift Detected. Rxy less than Threshold.
49	2616.10	91.55	No Doppler Shift. df/dt inadmissible.
50	2632.81	109.86	No Doppler Shift Detected. Rxy less than Threshold.
51	2635.76	97.66	No Doppler Shift Detected. Rxy less than Threshold.
52	2642.64	106.81	No Doppler Shift Detected. Rxy less than Threshold.
53	2656.40	97.66	No Doppler Shift. df/dt inadmissible.
54	2692.78	161.74	No Doppler Shift. df/dt inadmissible.
55	2716.54	106.81	No Doppler Shift. df/dt inadmissible.
56	2733.25	97.66	No Doppler Shift. df/dt inadmissible.
57	2735.22	125.12	No Doppler Shift. df/dt inadmissible.
58	2739.15	125.12	No Doppler Shift. df/dt inadmissible.
59	2790.27	112.92	No Doppler Shift Detected. Rxy less than Threshold.
60	2796.17	91.55	No Doppler Shift. df/dt inadmissible.
61	2812.88	94.60	No Doppler Shift Detected. Rxy less than Threshold.
62	2822.71	91.55	No Doppler Shift Detected. Rxy less than Threshold.
63	2825.66	115.97	No Doppler Shift. df/dt inadmissible.
64	2849.25	112.92	No Doppler Shift Detected. Rxy less than Threshold.
65	2865.96	125.12	No Doppler Shift. df/dt inadmissible.
66	2873.83	91.55	No Doppler Shift. df/dt inadmissible.
67	2882.68	91.55	No Doppler Shift Detected. Rxy less than Threshold.
68	2920.03	97.66	No Doppler Shift. df/dt inadmissible.
69	2938.71	106.81	No Doppler Shift Detected. Rxy less than Threshold.
70	2943.62	97.66	No Doppler Shift Detected. Rxy less than Threshold.
71	2948.54	91.55	No Doppler Shift Detected. Rxy less than Threshold.
72	2983.93	125.12	No Doppler Shift. df/dt inadmissible.
73	2987.86	91.55	No Doppler Shift Detected. Rxy less than Threshold.
74	3008.68	97.66	No Doppler Shift Detected. Rxy less than Threshold.
75	3013.59	100.71	No Doppler Shift Detected. Rxy less than Threshold.
76	3023.42	91.55	No Doppler Shift Detected. Rxy less than Threshold.
77	3041.12	91.55	No Doppler Shift Detected. Rxy less than Threshold.
78	3048.00	112.92	No Doppler Shift Detected. Rxy less than Threshold.
79	3050.95	128.17	No Doppler Shift Detected. Rxy less than Threshold.
80	3056.85	122.07	No Doppler Shift Detected. Rxy less than Threshold.
81	3060.78	94.60	No Doppler Shift Detected. Rxy less than Threshold.

82	3069.63	91.55	No Doppler Shift. df/dt inadmissible.			
83	3073.56	103.76	No Doppler Shift Detected. Rxy less than Threshold.			
84	3075.52	91.55	No Doppler Shift Detected. Rxy less than Threshold.			
85	3078.47	115.97	No Doppler Shift Detected. Rxy less than Threshold.			
86	3083.39	100.71	No Doppler Shift Detected. Rxy less than Threshold.			
87	3095.19	122.07	No Doppler Shift Detected. Rxy less than Threshold.			
88	3105.02	91.55	No Doppler Shift Detected. Rxy less than Threshold.			
89	3113.86	125.12	Contact with Doppler Shift found.	50.42	18.28	35.14
90	3121.73	97.66	No Doppler Shift Detected. Rxy less than Threshold.			
91	3204.30	112.92	No Doppler Shift Detected. Rxy less than Threshold.			
92	3209.22	97.66	No Doppler Shift Detected. Rxy less than Threshold.			
93	3262.30	97.66	No Doppler Shift Detected. Rxy less than Threshold.			
94	3264.27	91.55	No Doppler Shift. df/dt inadmissible.			
95	3278.03	106.81	No Doppler Shift Detected. Rxy less than Threshold.			
96	3280.98	106.81	No Doppler Shift Detected. Rxy less than Threshold.			
97	3286.88	97.66	No Doppler Shift Detected. Rxy less than Threshold.			
98	3292.78	115.97	No Doppler Shift Detected. Rxy less than Threshold.			
99	3300.81	125.12	No Doppler Shift. df/dt inadmissible.			
100	3303.76	91.55	No Doppler Shift Detected. Rxy less than Threshold.			
101	3389.29	100.71	No Doppler Shift. df/dt inadmissible.			
102	3443.35	97.66	No Doppler Shift Detected. Rxy less than Threshold.			
103	3447.29	125.12	No Doppler Shift. df/dt inadmissible.			
104	3451.22	161.74	No Doppler Shift. df/dt inadmissible.			
105	3456.13	100.71	No Doppler Shift. df/dt inadmissible.			
106	3461.05	97.66	No Doppler Shift Detected. Rxy less than Threshold.			
107	3463.02	125.12	No Doppler Shift. df/dt inadmissible.			
108	3485.62	125.12	No Doppler Shift. df/dt inadmissible.			
109	3489.56	112.92	No Doppler Shift Detected. Rxy less than Threshold.			
110	3511.18	109.86	No Doppler Shift Detected. Rxy less than Threshold.			
111	3516.10	109.86	No Doppler Shift Detected. Rxy less than Threshold.			
112	3526.91	115.97	No Doppler Shift Detected. Rxy less than Threshold.			
113	3622.44	125.12	No Doppler Shift. df/dt inadmissible.			

4. Run 4 – Threshold μ + 20σ, Rxy Threshold $\mu_r + 1.0\sigma_r$

Results from analysis of 07_aug_08.txt.

Threshold for energy based detection = 0.1380.
No of peaks found = 113.
No of Doppler Shifts detected = 5.

Start time : 8/7/2008 10:20:52.55.

Peak No.	Time	Freq	Result	Velocity	Rxy	Range	
1	74.71	122.07	Contact with Doppler Shift found.		48.26	56.43	106.80
2	623.42	94.60	Contact with Doppler Shift found.		53.33	51.63	168.48
3	814.13	125.12	No Doppler Shift. df/dt inadmissible.				
4	816.10	91.55	No Doppler Shift Detected. Rxy less than Threshold.				
5	818.07	122.07	No Doppler Shift. df/dt inadmissible.				
6	822.98	103.76	No Doppler Shift Detected. Rxy less than Threshold.				
7	835.76	115.97	No Doppler Shift Detected. Rxy less than Threshold.				
8	1089.56	103.76	No Doppler Shift Detected. Rxy less than Threshold.				
9	1092.51	109.86	No Doppler Shift. df/dt inadmissible.				
10	1215.56	112.92	No Doppler Shift. df/dt inadmissible.				
11	1273.56	100.71	No Doppler Shift Detected. Rxy less than Threshold.				
12	1276.51	115.97	No Doppler Shift. df/dt inadmissible.				
13	1422.98	112.92	No Doppler Shift Detected. Rxy less than Threshold.				
14	1430.84	106.81	No Doppler Shift. df/dt inadmissible.				
15	1457.39	91.55	No Doppler Shift Detected. Rxy less than Threshold.				
16	1519.49	103.76	No Doppler Shift Detected. Rxy less than Threshold.				
17	1521.46	106.81	No Doppler Shift Detected. Rxy less than Threshold.				
18	1524.41	91.55	No Doppler Shift Detected. Rxy less than Threshold.				
19	1575.52	122.07	No Doppler Shift. df/dt inadmissible.				
20	1582.41	137.33	Contact with Doppler Shift found.		61.11	47.38	321.10
21	1619.76	100.71	No Doppler Shift Detected. Rxy less than Threshold.				
22	1653.18	94.60	No Doppler Shift Detected. Rxy less than Threshold.				
23	1794.74	225.83	No Doppler Shift Detected. Rxy less than Threshold.				
24	1805.73	97.66	No Doppler Shift Detected. Rxy less than Threshold.				
25	1811.63	91.55	No Doppler Shift Detected. Rxy less than Threshold.				
26	1872.58	125.12	No Doppler Shift. df/dt inadmissible.				
27	1874.54	97.66	No Doppler Shift. df/dt inadmissible.				
28	1924.68	137.33	Contact with Doppler Shift found.		48.15	30.36	85.42
29	1931.56	109.86	No Doppler Shift. df/dt inadmissible.				
30	1943.35	97.66	No Doppler Shift Detected. Rxy less than Threshold.				
31	1946.30	134.28	No Doppler Shift Detected. Rxy less than Threshold.				
32	1957.12	94.60	No Doppler Shift. df/dt inadmissible.				
33	2004.30	125.12	No Doppler Shift. df/dt inadmissible.				
34	2028.88	109.86	No Doppler Shift Detected. Rxy less than Threshold.				

35	2119.49	131.23	Contact with Doppler Shift found.	44.00	46.24	119.29
36	2214.85	91.55	No Doppler Shift Detected. Rxy less than Threshold.			
37	2216.81	97.66	No Doppler Shift Detected. Rxy less than Threshold.			
38	2229.59	91.55	No Doppler Shift Detected. Rxy less than Threshold.			
39	2232.54	125.12	No Doppler Shift. df/dt inadmissible.			
40	2263.02	91.55	No Doppler Shift. df/dt inadmissible.			
41	2269.90	94.60	No Doppler Shift Detected. Rxy less than Threshold.			
42	2301.35	161.74	No Doppler Shift. df/dt inadmissible.			
43	2305.29	119.02	No Doppler Shift Detected. Rxy less than Threshold.			
44	2311.18	100.71	No Doppler Shift Detected. Rxy less than Threshold.			
45	2371.15	91.55	No Doppler Shift Detected. Rxy less than Threshold.			
46	2467.66	100.71	No Doppler Shift Detected. Rxy less than Threshold.			
47	2601.35	97.66	No Doppler Shift. df/dt inadmissible.			
48	2611.18	91.55	No Doppler Shift Detected. Rxy less than Threshold.			
49	2616.10	91.55	No Doppler Shift. df/dt inadmissible.			
50	2632.81	109.86	No Doppler Shift Detected. Rxy less than Threshold.			
51	2635.76	97.66	No Doppler Shift Detected. Rxy less than Threshold.			
52	2642.64	106.81	No Doppler Shift Detected. Rxy less than Threshold.			
53	2656.40	97.66	No Doppler Shift. df/dt inadmissible.			
54	2692.78	161.74	No Doppler Shift. df/dt inadmissible.			
55	2716.54	106.81	No Doppler Shift. df/dt inadmissible.			
56	2733.25	97.66	No Doppler Shift. df/dt inadmissible.			
57	2735.22	125.12	No Doppler Shift. df/dt inadmissible.			
58	2739.15	125.12	No Doppler Shift. df/dt inadmissible.			
59	2790.27	112.92	No Doppler Shift Detected. Rxy less than Threshold.			
60	2796.17	91.55	No Doppler Shift. df/dt inadmissible.			
61	2812.88	94.60	No Doppler Shift Detected. Rxy less than Threshold.			
62	2822.71	91.55	No Doppler Shift Detected. Rxy less than Threshold.			
63	2825.66	115.97	No Doppler Shift. df/dt inadmissible.			
64	2849.25	112.92	No Doppler Shift Detected. Rxy less than Threshold.			
65	2865.96	125.12	No Doppler Shift. df/dt inadmissible.			
66	2873.83	91.55	No Doppler Shift. df/dt inadmissible.			
67	2882.68	91.55	No Doppler Shift Detected. Rxy less than Threshold.			
68	2920.03	97.66	No Doppler Shift. df/dt inadmissible.			
69	2938.71	106.81	No Doppler Shift Detected. Rxy less than Threshold.			
70	2943.62	97.66	No Doppler Shift Detected. Rxy less than Threshold.			
71	2948.54	91.55	No Doppler Shift Detected. Rxy less than Threshold.			
72	2983.93	125.12	No Doppler Shift. df/dt inadmissible.			
73	2987.86	91.55	No Doppler Shift Detected. Rxy less than Threshold.			
74	3008.68	97.66	No Doppler Shift Detected. Rxy less than Threshold.			
75	3013.59	100.71	No Doppler Shift Detected. Rxy less than Threshold.			
76	3023.42	91.55	No Doppler Shift Detected. Rxy less than Threshold.			
77	3041.12	91.55	No Doppler Shift Detected. Rxy less than Threshold.			
78	3048.00	112.92	No Doppler Shift Detected. Rxy less than Threshold.			
79	3050.95	128.17	No Doppler Shift Detected. Rxy less than Threshold.			
80	3056.85	122.07	No Doppler Shift Detected. Rxy less than Threshold.			

81	3060.78	94.60	No Doppler Shift Detected. Rxy less than Threshold.
82	3069.63	91.55	No Doppler Shift. df/dt inadmissible.
83	3073.56	103.76	No Doppler Shift Detected. Rxy less than Threshold.
84	3075.52	91.55	No Doppler Shift Detected. Rxy less than Threshold.
85	3078.47	115.97	No Doppler Shift Detected. Rxy less than Threshold.
86	3083.39	100.71	No Doppler Shift Detected. Rxy less than Threshold.
87	3095.19	122.07	No Doppler Shift Detected. Rxy less than Threshold.
88	3105.02	91.55	No Doppler Shift Detected. Rxy less than Threshold.
89	3113.86	125.12	No Doppler Shift Detected. Rxy less than Threshold.
90	3121.73	97.66	No Doppler Shift Detected. Rxy less than Threshold.
91	3204.30	112.92	No Doppler Shift Detected. Rxy less than Threshold.
92	3209.22	97.66	No Doppler Shift Detected. Rxy less than Threshold.
93	3262.30	97.66	No Doppler Shift Detected. Rxy less than Threshold.
94	3264.27	91.55	No Doppler Shift. df/dt inadmissible.
95	3278.03	106.81	No Doppler Shift Detected. Rxy less than Threshold.
96	3280.98	106.81	No Doppler Shift Detected. Rxy less than Threshold.
97	3286.88	97.66	No Doppler Shift Detected. Rxy less than Threshold.
98	3292.78	115.97	No Doppler Shift Detected. Rxy less than Threshold.
99	3300.81	125.12	No Doppler Shift. df/dt inadmissible.
100	3303.76	91.55	No Doppler Shift Detected. Rxy less than Threshold.
101	3389.29	100.71	No Doppler Shift. df/dt inadmissible.
102	3443.35	97.66	No Doppler Shift Detected. Rxy less than Threshold.
103	3447.29	125.12	No Doppler Shift. df/dt inadmissible.
104	3451.22	161.74	No Doppler Shift. df/dt inadmissible.
105	3456.13	100.71	No Doppler Shift. df/dt inadmissible.
106	3461.05	97.66	No Doppler Shift Detected. Rxy less than Threshold.
107	3463.02	125.12	No Doppler Shift. df/dt inadmissible.
108	3485.62	125.12	No Doppler Shift. df/dt inadmissible.
109	3489.56	112.92	No Doppler Shift Detected. Rxy less than Threshold.
110	3511.18	109.86	No Doppler Shift Detected. Rxy less than Threshold.
111	3516.10	109.86	No Doppler Shift Detected. Rxy less than Threshold.
112	3526.91	115.97	No Doppler Shift Detected. Rxy less than Threshold.
113	3622.44	125.12	No Doppler Shift. df/dt inadmissible.

5. Run 5 – Threshold μ + 15σ, Rxy Threshold $\mu_r + 0.5\sigma_r$

Results from analysis of 07_aug_08.txt.

Threshold for energy based detection = 0.3000.
No of peaks found = 65.
No of Doppler Shifts detected = 5.

Start time : 8/7/2008 10:20:52.55.

Peak No.	Time	Freq	Result	Velocity	Rxy	Range		
1	74.71	122.07	Contact with Doppler Shift found.	48.26	56.43	106.80		
2	623.42	94.60	Contact with Doppler Shift found.	53.33	51.63	168.48		
3	1276.51	115.97	No Doppler Shift. df/dt inadmissible.					
4	1422.98	112.92	No Doppler Shift Detected. Rxy less than Threshold.					
5	1427.90	94.60	No Doppler Shift Detected. Rxy less than Threshold.					
6	1524.41	91.55	No Doppler Shift Detected. Rxy less than Threshold.					
7	1580.44	170.90	Contact with Doppler Shift found.	46.97	41.53	177.04		
8	1582.41	149.54	Contact with Doppler Shift found.	61.11	47.38	321.10		
9	1653.18	94.60	No Doppler Shift Detected. Rxy less than Threshold.					
10	1924.68	137.33	Contact with Doppler Shift found.	48.15	30.36	85.42		
11	1927.63	112.92	No Doppler Shift Detected. Rxy less than Threshold.					
12	1929.59	91.55	No Doppler Shift Detected. Rxy less than Threshold.					
13	1931.56	109.86	No Doppler Shift. df/dt inadmissible.					
14	1933.52	109.86	No Doppler Shift. df/dt inadmissible.					
15	1935.49	100.71	No Doppler Shift Detected. Rxy less than Threshold.					
16	2214.85	91.55	No Doppler Shift Detected. Rxy less than Threshold.					
17	2216.81	97.66	No Doppler Shift Detected. Rxy less than Threshold.					
18	2229.59	91.55	No Doppler Shift Detected. Rxy less than Threshold.					
19	2259.08	100.71	No Doppler Shift Detected. Rxy less than Threshold.					
20	2263.02	91.55	No Doppler Shift. df/dt inadmissible.					
21	2269.90	94.60	No Doppler Shift Detected. Rxy less than Threshold.					
22	2301.35	161.74	No Doppler Shift. df/dt inadmissible.					
23	2305.29	119.02	No Doppler Shift Detected. Rxy less than Threshold.					
24	2311.18	100.71	No Doppler Shift Detected. Rxy less than Threshold.					
25	2467.66	100.71	No Doppler Shift Detected. Rxy less than Threshold.					
26	2601.35	97.66	No Doppler Shift. df/dt inadmissible.					
27	2611.18	91.55	No Doppler Shift Detected. Rxy less than Threshold.					
28	2616.10	91.55	No Doppler Shift. df/dt inadmissible.					
29	2635.76	97.66	No Doppler Shift Detected. Rxy less than Threshold.					
30	2642.64	106.81	No Doppler Shift Detected. Rxy less than Threshold.					
31	2716.54	106.81	No Doppler Shift. df/dt inadmissible.					
32	2790.27	112.92	No Doppler Shift Detected. Rxy less than Threshold.					
33	2793.22	106.81	No Doppler Shift Detected. Rxy less than Threshold.					
34	2796.17	91.55	No Doppler Shift. df/dt inadmissible.					

35	2815.83	94.60	No Doppler Shift Detected. Rxy less than Threshold.
36	2822.71	91.55	No Doppler Shift Detected. Rxy less than Threshold.
37	2830.57	106.81	No Doppler Shift Detected. Rxy less than Threshold.
38	2833.52	91.55	No Doppler Shift Detected. Rxy less than Threshold.
39	2849.25	112.92	No Doppler Shift Detected. Rxy less than Threshold.
40	2873.83	91.55	No Doppler Shift. df/dt inadmissible.
41	2882.68	91.55	No Doppler Shift Detected. Rxy less than Threshold.
42	2884.64	97.66	No Doppler Shift Detected. Rxy less than Threshold.
43	2943.62	97.66	No Doppler Shift Detected. Rxy less than Threshold.
44	2948.54	91.55	No Doppler Shift Detected. Rxy less than Threshold.
45	2950.51	106.81	No Doppler Shift. df/dt inadmissible.
46	2952.47	91.55	No Doppler Shift Detected. Rxy less than Threshold.
47	2987.86	91.55	No Doppler Shift Detected. Rxy less than Threshold.
48	3002.78	112.92	No Doppler Shift Detected. Rxy less than Threshold.
49	3008.68	97.66	No Doppler Shift Detected. Rxy less than Threshold.
50	3023.42	91.55	No Doppler Shift Detected. Rxy less than Threshold.
51	3041.12	91.55	No Doppler Shift Detected. Rxy less than Threshold.
52	3043.08	97.66	No Doppler Shift. df/dt inadmissible.
53	3048.00	112.92	No Doppler Shift Detected. Rxy less than Threshold.
54	3050.95	128.17	No Doppler Shift Detected. Rxy less than Threshold.
55	3060.78	94.60	No Doppler Shift Detected. Rxy less than Threshold.
56	3078.47	115.97	No Doppler Shift Detected. Rxy less than Threshold.
57	3095.19	122.07	No Doppler Shift Detected. Rxy less than Threshold.
58	3111.90	112.92	No Doppler Shift Detected. Rxy less than Threshold.
59	3113.86	125.12	No Doppler Shift Detected. Rxy less than Threshold.
60	3121.73	97.66	No Doppler Shift Detected. Rxy less than Threshold.
61	3278.03	106.81	No Doppler Shift Detected. Rxy less than Threshold.
62	3292.78	115.97	No Doppler Shift Detected. Rxy less than Threshold.
63	3456.13	100.71	No Doppler Shift. df/dt inadmissible.
64	3516.10	109.86	No Doppler Shift Detected. Rxy less than Threshold.
65	3526.91	115.97	No Doppler Shift Detected. Rxy less than Threshold.

LIST OF REFERENCES

ACO Pacific Inc. (n.d.). *ACOtron™ Preamp Specifications, 4012 Family.* [Brochure]. Retrieved from http://www.acopacific.com/acotrndt.html#4012 on 12 Feb 2009.

Flightaware. (n.d.). [Search term: Monterey Airport]. Retrieved from http://flightaware.com/live/airport/KMRY on 7 Aug 2008.

Green, D.M., & Swets J.M. (1966). *Signal Detection Theory and Psychophysics*. New York: John Wiley and Sons.

Kindsler, L. E., Frey, A. R, Coppens, A. B., & Sanders, J. V. (2000). *Fundamentals of Acoustics.* (5th ed.) New York: John Wiley and Sons.

Le Chevalier, F. (2002). *Principles of Radar and Sonar Signal Processing*. Boston: Artech House, p. 15.

Lurton, X. (2002). *An Introduction to Underwater Acoustics – Principles and Applications*. Chichester, UK: Praxis Publishing.

Mapquest. (n.d). [Search term: Naval Postgraduate School, Monterey, CA]. Retrieved from http://www.mapquest.com on 10 Feb 2009.

National Instruments. (n.d.). *NI USB-9233 Technical Specifications.* [Brochure]. Retrieved from http://www.ni.com/pdf/products/us/20066578101d.pdf on 12 Feb 2009.

Smith, S. W. (1997). *The Scientist and Engineer's Guide to Digital Signal Processing*. San Diego: California Technical Publishing.

Urick, R. J. (1983). *Principles of Underwater Sound.* (3rd ed.) Los Altos: Peninsula Publishing.

Wagner, D. H., Mylander W. C, & Sanders, T. J. (1999). *Naval Operations Analysis*. Annapolis: Naval Institute Press, p. 118.

Washburn, A. R. (2002). *Search and Detection.* (4th ed.) Linthicum: Institute for Operations Research and the Management Sciences.

Ziomek, L. J. (1994). *Fundamentals of Acoustic Field Theory and Space-Time Signal Processing.* Boca Raton: CRC Press, p. 622.

THIS PAGE INTENTIONALLY LEFT BLANK

INITIAL DISTRIBUTION LIST

1. Defense Technical Information Center
   Ft. Belvoir, Virginia

2. Dudley Knox Library
   Naval Postgraduate School
   Monterey, California

3. Professor Daphne Kapolka
   Naval Postgraduate School
   Monterey, California

4. Professor Joseph Rice
   Naval Postgraduate School
   Monterey, California

5. RADM (Ret) Ray Jones
   Naval Postgraduate School
   Monterey, California

6. RADM (Ret) Rick Williams
   Naval Postgraduate School
   Monterey, California

7. RADM (Ret) Winford Ellis
   Naval Postgraduate School
   Monterey, California

8. LCDR Victoria Taber
   Naval Postgraduate School
   Monterey, California

9. LT Jeremy Biediger
   Naval Postgraduate School
   Monterey, California

10. MAJ Goh, Meng Chong
    Naval Postgraduate School
    Monterey, California

11. Dr. Paul Gendron
    SPAWAR Systems Centre Pacific
    San Diego, California